



Characteristics of the Cretaceous Magmatism in Huanghua Depression and Their Relationships with Hydrocarbon Enrichment


Fengming Jin¹, Jian Huang^{1,2,3}, Xiugang Pu¹, Changqian Ma^{1,2,3}, Lixin Fu¹,
Chongbiao Leng^{2,3}, Da Lou¹, Mutian Qin^{2,3}

1. Dagang Oilfield Company, China National Petroleum Corporation, Tianjin 300280, China

2. State Key Laboratory of Geological Processes and Mineral Resources, China University of Geosciences, Wuhan 430078, China

3. School of Earth Sciences, China University of Geosciences, Wuhan 430074, China

 Fengming Jin: <https://orcid.org/0000-0002-3153-3331>;  Jian Huang: <https://orcid.org/0000-0001-6384-3388>;

 Changqian Ma: <https://orcid.org/0000-0002-1778-0547>

ABSTRACT: The Huanghua depression located in the hinterland of the Bohai Bay Basin in eastern China is a typical area for the research of multistage magmatic activities with hydrocarbon enrichment, many high-yield wells related to igneous rocks were discovered within the Cretaceous strata in recent years. However, the spatial and temporal distribution of Cretaceous igneous rocks remains unclear, and the relationships among magmatic sequence, lithology, and hydrocarbon enrichment have been poorly studied. In order to solve these problems, core observation, logging analysis, major element analysis, zircon U-Pb chronology, oil-bearing grade statistics and reservoir spaces analysis were used to subdivide the magmatism cycles and to investigate the characteristics of igneous reservoirs. Our results show that the Mesozoic magmatism in Huanghua depression started in 140.1 ± 1.4 Ma and could be divided into two stages including the Early Cretaceous stage and Late Cretaceous stage. The Early Cretaceous magmatism principally developed basic-intermediate rocks in the north zone, and could be subdivided into 3 cycles with their forming ages of 140, 125–119, and 118–111 Ma, respectively. By contrast, the late stage mainly developed intermediate-acid rocks centralized in the south zone and formed at 75–70 Ma. The GR and SP curves are good indicators for the contrast of different lithologies, lithofacies and for magmatic sequences division. Intensive magmatism may have an advantage to form reservoirs, since basalt in cycle III in the Early Cretaceous and dacite porphyrite in the Late Cretaceous have great exploration potential. Lithology and tectonic fractures have an important influence on the formation of reservoir spaces and hydrocarbon enrichment. The characteristics of Cretaceous magmatism and igneous reservoirs in Huanghua depression and adjacent areas are summarized, providing important information for igneous reservoirs research and oil-gas exploration in the Cretaceous in related areas.

KEY WORDS: Cretaceous magmatism, magmatic sequences division, igneous reservoir, hydrocarbon enrichment, Huanghua depression, oil-gas reservoir space.

0 INTRODUCTION

Volcanic accumulation of oil and gas has been a new global field of hydrocarbon exploration since the discovery of volcanic reservoirs in the San Joaquin Basin of California in the United States at the end of the 19th century. Nowadays more than 300 occurrences of hydrocarbon accumulation related to igneous rocks in more than 20 countries and regions have been confirmed (Zou et al., 2013; Schutter, 2003). Previous studies show that the

evolution and hydrocarbon-bearing capacity of basins are closely related to volcanic activity with significant reservoirs discovered in igneous rocks (Wen et al., 2019; Wang and Chen, 2015; Gu et al., 2002). In the last 30 years, researches and explorations have been carried out in Sichuan, Junggar, Songliao, Santanhu and Bohai Bay basins in China, and many igneous reservoirs of different sizes have been discovered (Ma et al., 2019; Xie et al., 2019; Wang G et al., 2018). Great achievements have been obtained in theories and explorations of igneous hydrocarbon enrichment in recent years. For example, the theory that “entire volcanic structure contains oil” was invoked for the exploration in the Junggar Basin, and confirmed that the oil reserve scale of the Hongche fault zone related to the Carboniferous igneous rock was over one hundred million tons (He et al., 2019). Moreover, both proven natural gas reserves in the Songliao Basin related to Cretaceous igneous rocks and the Sichuan Basin related to Per-

*Corresponding author: huangjian@cug.edu.cn;
cqma@cug.edu.cn

© China University of Geosciences (Wuhan) and Springer-Verlag GmbH Germany, Part of Springer Nature 2020

Manuscript received August 10, 2020.

Manuscript accepted October 31, 2020.

mian igneous rocks exceeded $2.5 \times 10^8 \text{ m}^3$ (He et al., 2019; Feng et al., 2014), confirming the great potential for the exploration and development of igneous reservoirs.

The Bohai Bay Basin located in the eastern margin of the North China Craton developed many Mesozoic and Cenozoic reservoirs (Zhang J L et al., 2019), and gave side to exploration and development of igneous reservoirs there started more than 50 years ago. More than 30 igneous reservoir occurrences and over ten million tons of oil reservoirs confirm the great exploration potential of igneous reservoirs (Yang et al., 2017). The principal areas with igneous reservoirs include the Bohai Sea area, Liaohe, Huanghua, and Jiyang depressions (Cai et al., 2018). Previous exploration results in the Liaohe depression confirmed that the igneous related oil reserves exceeded $4.317 \times 10^4 \text{ t}$ in the depression (Mu, 2015), principal lithologies were acid-intermediate rocks in Mesozoic, and the high-productivity well in the Xing-longtai area in the western sag has achieved $80 \times 10^4 \text{ m}^3$ daily gas production and 110 t oil production, respectively (Li et al., 2012). In the Bohai Sea area, before 2010 researches were mainly focused on the lithologies identification of igneous reservoirs, and in recent years, great progress was made on the volcanic apparatus and many multiple hydrocarbon structures such as 428W, B22-2, and Q30-1 (Wu et al., 2017; Ye et al., 2017) have been discovered. In the Huanghua depression, several high yield wells with more than 100 t daily production were discovered in the Wangguantun and Fenghuadian areas, and the proved reserves in Cretaceous strata were higher than other strata (Zheng and You, 2019).

The study area, Huanghua depression, is a Meso–Cenozoic fault depression tectonic unit located in the hinterland of the Bohai Bay Basin in eastern China. Previous studies mainly focus on the Cenozoic volcanic rocks, most of which are investigations into their distribution, reservoir space types, well logging technologies and the magmatic effects on oil and gas generation (Zhou et al., 2020; Gao et al., 2015; Mao et al., 2015; Li et al., 2014; Luo et al., 1996). Studies on the Early Cretaceous igneous rocks in the Huanghua depression and the Bohai Bay Basin were mostly related to either their reservoir characteristics (Jin et al., 2013) or implications for the Yanshanian movement (Zhu et al., 2019; Zuo et al., 2015; Zhang et al., 2011). Only a few studies mentioned the Late Cretaceous magmatism (Zheng and You, 2019; Zhu et al., 2019). Even so, no much attention has been paid to the spatial-temporal distribution of igneous rocks and their relation to hydrocarbon accumulation. Therefore, several key problems still need to be studied for oil-gas exploration, including how the Cretaceous igneous rocks are distributed in the Huanghua depression? which strata of igneous rocks are beneficial to oil and gas accumulation? and which lithologies and lithofacies are easy to become reservoirs?

In this study, the authors aim to clarify the magmatic sequence and distribution of Cretaceous igneous rocks, and put forward the new understanding of the relationships among the magmatic sequence, lithology, and hydrocarbon enrichment in the Huanghua depression.

1 GEOLOGICAL BACKGROUND

The famous Mesozoic Yanshanian movement occurred in Mesozoic was an important tectonic event accompanied by extensive magmatic activities and the formation of petroliferous

basins, it significantly influenced the tectonic deformation of the North China Craton and formed the present-day tectonic framework and topography of eastern China and even the East Asia (Zhang et al., 2020; Dong et al., 2018; Wong, 1929). Though heated debates remain over the dynamic mechanism and episodes division, most scholars agreed that the westward subduction of the Pacific Plate has a great influence on the Yanshanian movement (Zhang et al., 2020; Wang Y et al., 2018; Zhao et al., 2004). Previous researches indicated the Yanshanian movement began with intensive intra-continental contraction in Jurassic (from $\sim 170 \pm 5 \text{ Ma}$). The alternating stages of crustal shortening at ~ 170 – 136 Ma reflected in the generation of two regional stratigraphic unconformities (the Tiaojishan and Zhangjiakou unconformities), which were initially named the A and B episodes of “the Yanshan Orogeny” by Mr. Wenhao Wong (Dong et al., 2018; Wong, 1929). After that, in the Cretaceous, extension collapse and lithospheric thinning (135–90 Ma) gave rise to the upwelling of asthenosphere mantle and resulted in massive magma intrusions and volcanic eruptions. As a result, thick layers of magmatic rocks developed in the late Early Cretaceous and a small amount of magmatic activity occurred in the Late Cretaceous (Ye et al., 2017; Kuang et al., 2012; Bing et al., 2003).

The NNE trend Mesozoic to Cenozoic Tanlu fault zone (Fig. 1a) with polyphase activities impacted the related areas including the formation and evolution of Bohai Bay Basin (Gong et al., 2007; Zhu et al., 2004). The study area, Huanghua depression, is a Meso–Cenozoic fault depression tectonic unit located in the hinterland of Bohai Bay Basin, series of NNE and NE folds and thrust tectonics were created accompanied with intensive compressional orogeny in the Late Jurassic and Early Cretaceous (Zhang F P et al., 2019; Fu et al., 2016), associated magma intruded the wall rocks or erupted to the surface along the NNE and NE faults in the Early Cretaceous (Zhou et al., 2012). The profile of the depression shows NE–SW trend was controlled by the tectonic faults, with Cangxian uplift bounded on the west, Chengning uplift on the east and Yanshan fold belt on the north, respectively (Fig. 1a). There are 26 buried hills within the Huanghua depression (Zhang J N et al., 2019), typical buried hills developed igneous rocks including Beitang, North Dagang, South Dagang, Koucun, Xianzhuang, Zaoyuan, Wangguantun, Yanshan and Xuhei areas (Fig. 1b). Basic, intermediate and acid lavas, tuffs and breccias were developed in Huanghua depression (Zhang et al., 2009). In this study, we focus on the igneous rocks developed in the central part of the Huanghua depression. To better describe their distribution, we named the North Dagang, South Dagang, Koucun and Xianzhuang areas as the north zone, and Wangguantun, Zaoyuan and Yanshan as the south zone.

2 PETROGRAPHY OF THE CRETACEOUS IGNEOUS ROCKS

According to the core samples, the principal igneous rock types in Huanghua depression include lava, pyroclastic and intrusive rocks; the main lithologies are basalt, andesite, dacite porphyrite, diabase, tuff, volcanoclastic rocks, tuffaceous sandstone and granite (Fig. 2).

The granite is mainly composed of orthoclase (35%–40%), plagioclase (25%–35%) and quartz (20%–35%), with minor

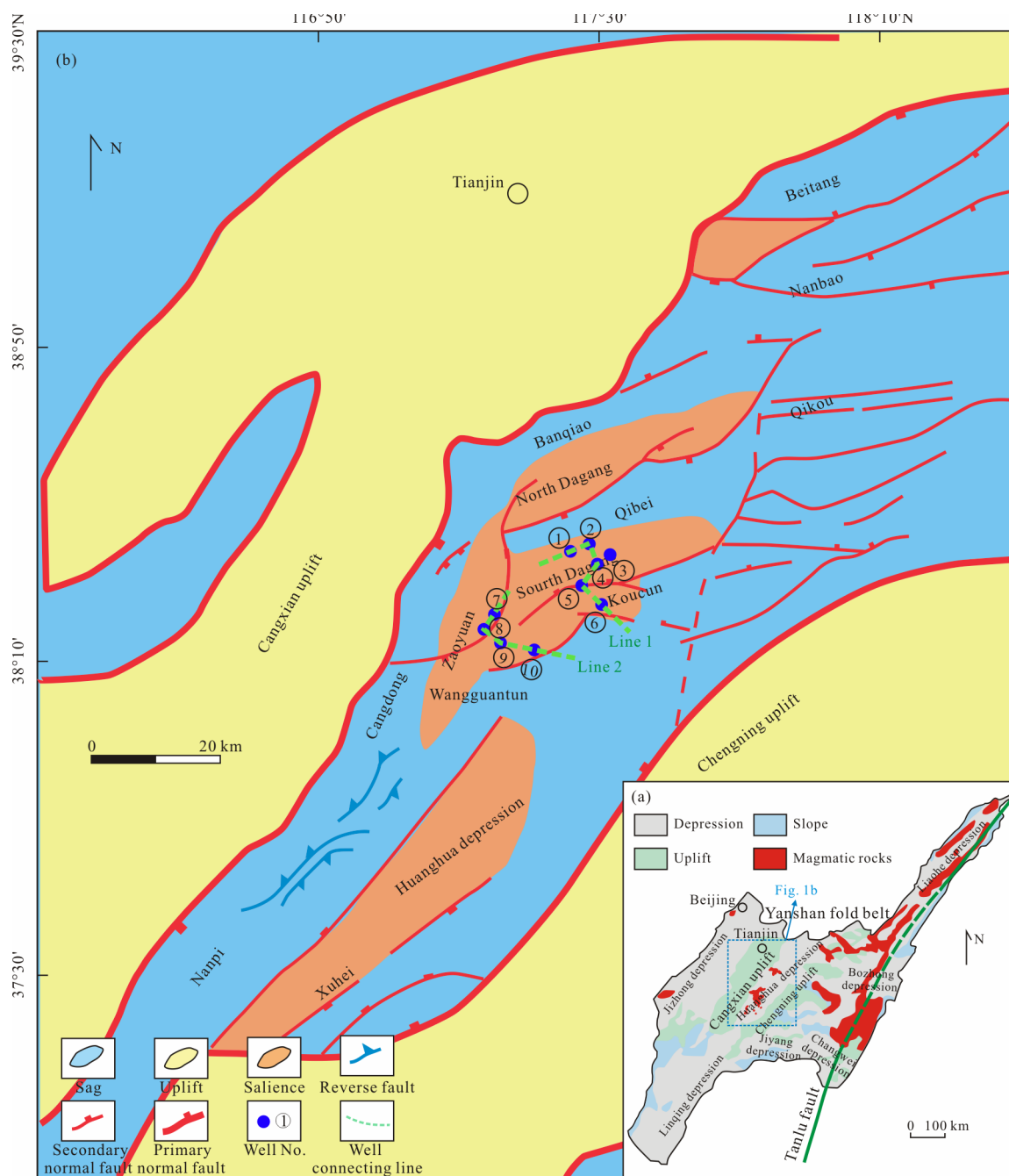


Figure 1. (a) Sketch map showing the Bohai Bay Basin, (b) structure map of the Huanghua depression (modified from Zhu et al., 2019). ① Well Qg101; ② Well Qg8; ③ Well Qg1601; ④ Well Qg2; ⑤ Well K36; ⑥ Well X6; ⑦ Well Z1531; ⑧ Well F22-15; ⑨ Well G177; ⑩ Well Y1; line 1 showing the cross section location of Fig. 7, and line 2 of Fig. 8.

biotite (2%–5%) and apatite. The orthoclases and plagioclases are subhedral, the quartzes are anhedral and biotites are flakes, most of the main minerals are 200 μm to 1 mm in size.

The dacite porphyry is dense massive structure and porphyritic texture, the rock samples are fresh, the phenocrysts include plagioclase, quartz and some biotite, mainly 200 to 600 μm in size. The groundmass is a cryptocrystalline texture and is composed of felsic minerals.

The andesite samples are strongly altered, vesicular and amygdaloidal structure and porphyritic texture, and the vesicles are \sim 500 μm to 2 mm in size. The main phenocrysts include plagioclase and amphibole, mainly 200–800 μm in size, and the

groundmass is mainly composed of microcrystalline plagioclase.

The basalt also has a similar structure and texture as andesite, but the phenocrysts are mainly iddingsites and pyroxenes. The iddingsites are the alteration products of olivines, they show the euhedral shapes of olivines and mainly 200–600 μm in size. The vesicles are suborbicular and 500 μm –2 mm in size.

The volcanoclastic rocks are composed of lava breccia and volcanic ash, the lava debris is 0.5 to 3 mm in size, quartz and sanidine clastics are easy to find in the lava breccias. The tuffaceous sandstone is composed of sediment and crystal clastics, the crystal clastics are relatively similar to those developed in lava debris but much smaller.

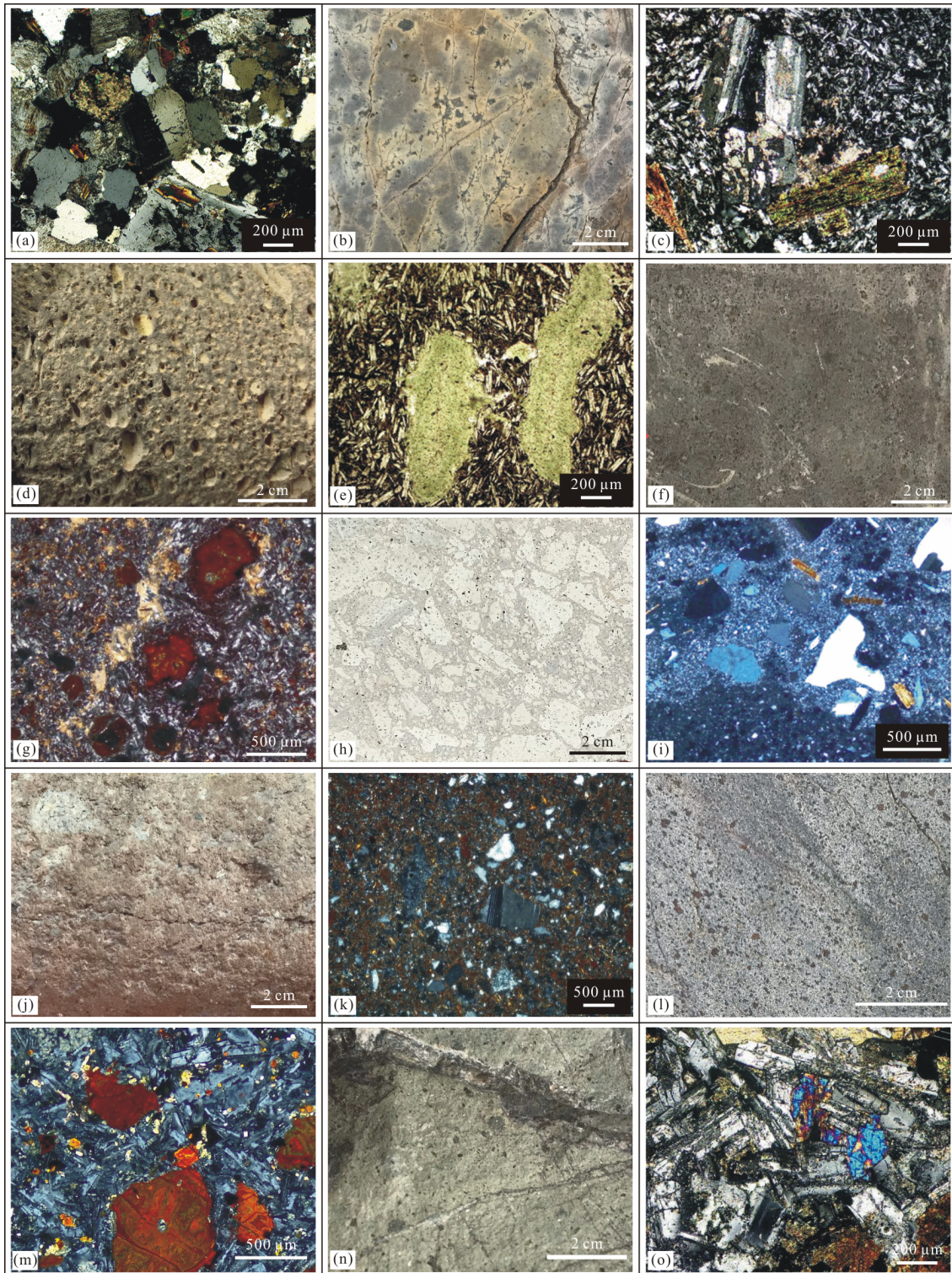


Figure 2. Photographs and microphotographs showing the typical core samples from Huanghua depression. (a) Well Y1, TVD 1 889 m, granite; (b), (c) Well F22-15, TVD 2 978 m, dacite porphyry; (d), (e) Well G177, TVD 2 308 m, andesite; (f), (g) Well K36, TVD 1 698 m, andesite; (h), (i) Well X6, TVD 2 171 m, volcanic breccia; (j), (k) Well Qg1601, TVD 2 778 m, tuffaceous sandstone; (l), (m) Well Qg2, TVD 2 325 m, basalt; (n) Well Qg8, TVD 3 372 m, andesitic porphyrite; (n), (o) Well Gs7, TVD 3 308 m, diabase.

The diabase is dense and fresh, mainly composed of plagioclase (60%–70%), clinopyroxene (15%–25%), and orthopyroxene (10%–15%). The plagioclases are euhedral and the clinopyroxene and orthopyroxene are subhedral, the minerals are similar in size, mainly 150–300 μm .

3 ANALYTICAL METHODS AND RESULTS

3.1 Sample Collection and Analytical Methods

3.1.1 Data and sample collection

To obtain a comprehensive understanding of the lithologic distribution, log data from 330 wells and 60 core samples from

28 drills in different areas of the depression were collected and analyzed. Besides, 12 cores from 11 wells were chosen for major element analysis, and 4 core samples from 3 wells for zircon U-Pb dating to subdivide the magmatism stages. Besides, oil-gas shows data were collected from 14 Early Cretaceous wells and 20 Late Cretaceous wells.

Core observation and major element analysis are used to classify the igneous lithologies, and then the lithology and log data are combined to map the rock distribution. After that, the chronology and stratigraphic charts are used to subdivide the magmatism cycles, and regional data are collected to discuss the relationship of reservoirs with magmatic sequences in the Huanghua depression and adjacent areas. In addition, the oil-bearing grades of different lithologies and typical reservoir spaces are discussed.

3.1.2 Whole-rock major elements analysis by XRF

Whole-rock major element concentrations were analyzed in the ALS Chemex (Guangzhou) Co., Ltd., by the X-ray fluorescence (XRF) analytical instrument (PANalytical PW2424), method code ME-XRF26d. A prepared sample (0.66 g) was fused with a 12 : 22 lithium tetraborate-lithium metaborate flux which also includes an oxidizing agent (lithium nitrate), and then poured into a platinum mold. The resultant disk was in turn analyzed by XRF spectrometry. The precision for most major elements was better than 5%.

3.1.3 *In-situ* U-Pb dating and trace element analysis of zircon grains by LA-ICP-MS

Zircon grains from wells Qg2, Qg8 and Qg101 were separated from crushed rocks using conventional magnetic and standard density methods. Representative zircons were hand-picked under a binocular microscope and then mounted in epoxy discs and polished. Transmitted and reflected light micrographs as well as cathodoluminescence (CL) images were obtained at Wuhan Sample Solution Analytical Technology Co., Ltd., Wuhan, China, to reveal the external and internal structures of the zircons.

Zircon U-Pb dating and trace element analyses were simultaneously conducted by LA-ICP-MS at Wuhan Sample Solution Analytical Technology Co., Ltd., Wuhan, China. Detailed operating conditions for the laser ablation system and the ICP-MS instrument and data reduction are the same as described by Zong et al. (2017). Laser sampling was performed using a GeolasPro laser ablation system that consists of a COMPexPro 102 ArF excimer laser (wavelength of 193 nm and maximum energy of 200 mJ) and a MicroLas optical system. An Agilent 7700e ICP-MS instrument was used to acquire ion-signal intensities. Helium was applied as a carrier gas. Argon was used as the make-up gas and mixed with the carrier gas via a T-connector before entering the ICP. A “wire” signal smoothing device is included in this laser ablation system (Hu et al., 2015). The spot size and frequency of the laser were set to 30 μm and 5 Hz, respectively. Zircon 91500 and glass NIST610 were used as external standards for U-Pb dating and trace element calibration, respectively. Each analysis incorporated a background acquisition of approximately 20–30 s followed by 50 s of data acquisition from the sample. An Excel-based software ICPMSDataCal was

used to perform off-line selection and integration of background and analyzed signals, time-drift correction and quantitative calibration for trace element analysis and U-Pb dating (Liu et al., 2010). Concordia diagrams and weighted mean calculations were made using Isoplot/Ex_ver3.

3.2 Results

3.2.1 Distribution and lithology of Cretaceous igneous rocks

Petrography examination and drilling position show that Cretaceous igneous rocks were generally controlled by faults in the Huanghua depression and distributed in NE-SW direction, within development focusing within the north zone (Fig. 3).

Andesites and basalts were the most widely distributed igneous rocks in the Huanghua depression. Basalts are more dominant type than andesites, especially in the north zone (Fig. 3a). Tuff and tuffaceous sandstones are co-occurred and mostly distributed in the north zone, while volcanoclastic rocks were concentrated in the southeast of Koucun and Xianzhuang areas (Fig. 3b). Dacite porphyrites mainly distributed in the Zaoyuan area of the south zone. Diabases dispersedly distributed in the north zone, and granites were sporadically discovered in the south zone (Fig. 3c).

The scales of Cretaceous igneous rocks are calculated based on thickness of log data, proportions of different lithologies, but are not very closely related to their distribution areas. The thickness of andesite layers is higher than that of basalts, which resulted in proportions of 42% and 34% for andesite and basalt, respectively. Tuffaceous sandstone, tuff, and volcanoclastic rocks show a very small proportion due to their thin layers. It should be pointed out that dacite porphyrite distributed in a small area and has a relatively large proportion of 12% (Fig. 3c), reflecting that the subvolcanic rock is thick in the south zone.

3.2.2 Major elements

The North Dagang and South Dagang rocks share similar lithologies. The major element data show that the most rock types are basic-intermediate rocks. For example, SiO_2 contents of North Dagang and South Dagang igneous rocks range from 47.97 wt.% to 56.98 wt.% (average 51.07 wt.%) with $\text{Na}_2\text{O}+\text{K}_2\text{O}$ of 5.50 wt.%–7.29 wt.% (average 6.54 wt.%), plotting mostly in the basaltic trachyandesite field above the boundary of alkaline series and subalkaline series in the TAS diagram (Fig. 4). Koucun volcanic rocks have a wide range of SiO_2 and $\text{Na}_2\text{O}+\text{K}_2\text{O}$, with 42.00 wt.%–60.06 wt.% (average 51.21 wt.%), and 4.48 wt.%–12.53 wt.% (average 7.27 wt.%), respectively, suggesting alkaline series for these rocks.

Acid volcanic rocks in the Zaoyuan area have high and relative narrow range of SiO_2 and $\text{Na}_2\text{O}+\text{K}_2\text{O}$, with 67.59 wt.%–72.51 wt.% (average 68.52 wt.%) and 8.66 wt.%–10.41 wt.% (average 9.33 wt.%), whereas, the Wangguantun volcanic rocks have relative low SiO_2 content (51.34 wt.% to 61.27 wt.%, with an average of 57.60 wt.%), but share similar $\text{Na}_2\text{O}+\text{K}_2\text{O}$ contents with those of Zaoyuan acid volcanic rocks.

3.2.3 *In-situ* zircon U-Pb ages

Four samples were selected from 3 wells in the South Dagang area to conduct *in-situ* U-Pb dating. The CL images and U-Pb ages are shown in Figs. 5 and 6, respectively.

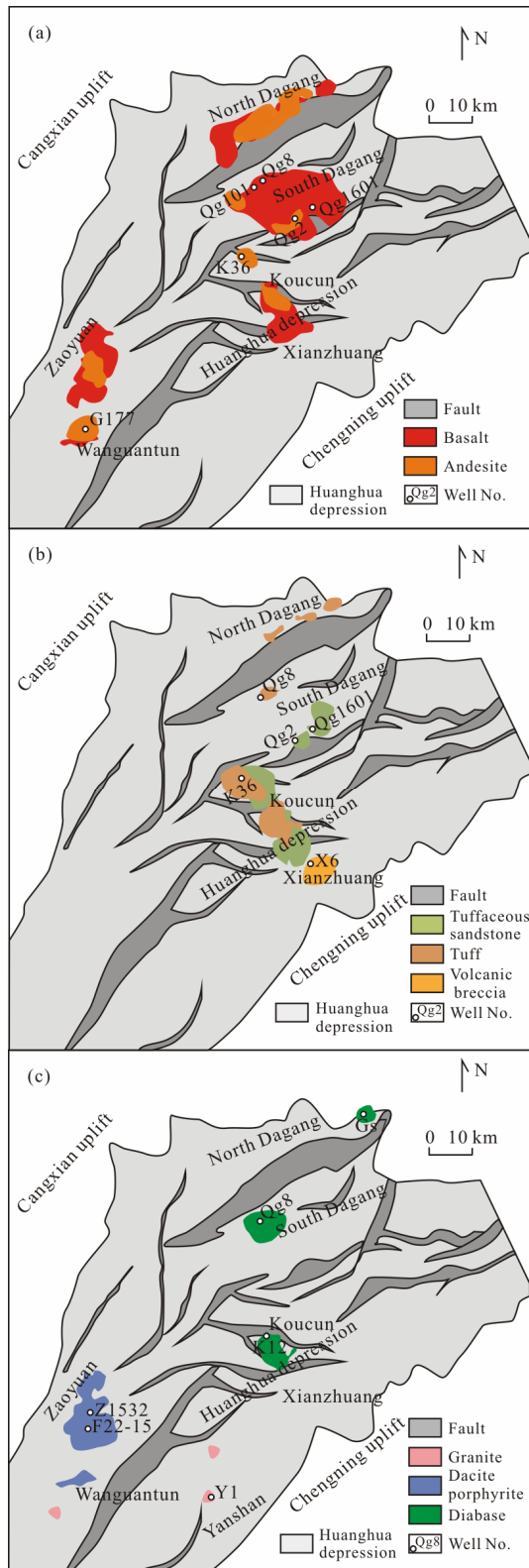


Figure 3. Distribution maps of Cretaceous igneous rocks in Huanghua depression based on cores and log data. The distribution of igneous rocks is closely related to the faults. (a) Basalt and andesite are widely distributed in the study area; (b) tuffaceous sandstone, tuff and volcanoclastic rocks are mainly distributed in the North Dagang and Koucun areas; (c) dacite porphyrite is concentrated in Zaoyuan in the south zone, granite and diabase are distributed sporadically in the study area.

The basalt sample Qg101-1 was collected from the 3 178–3 224 m depth of Well Qg101. Most zircon grains have length/width ratios of 1–3, with euhedral and rhythmic oscillatory zoning structure under CL images (Fig. 5a). Th/U ratios of the zircon grains range from 0.30 to 0.99 (average 0.57). These features suggest magmatic origin for these zircon grains. Thirteen valid analyses yield ages ranging from 110.0 to 118.2 Ma with mean $^{206}\text{Pb}/^{238}\text{U}$ age of 114.1 ± 1.4 Ma (MSWD=1.9) (Fig. 6a), which is interpreted as the crystallization age of the basalt.

The andesite Qg101-2 was collected from the 3 091–3 178 m depth in Well Qg101. The CL images display these zircons have 1–2 of length/width ratios and oscillatory zoning structure (Fig. 5b). Most zircon grains are euhedral prisms in morphology and some grains are fractured. Th/U ratios of these zircons vary from 0.29 to 1.18 with an average of 0.78. Seven valid analyses yield ages ranging from 113.0 to 119.9 Ma with a weighted mean $^{206}\text{Pb}/^{238}\text{U}$ age of 115.6 ± 4.7 Ma (MSWD=9.2) (Fig. 6b), which were interpreted as the crystallization age of the andesite.

The andesitic porphyrite Qg8 was sampled from the depth of 3 373.15 m in Well Qg8. Zircon grains from this sample have the length/width ratios of 1–5, and the CL images are characterized by a rhythmic oscillatory zoning structure (Fig. 5c). These grains have the Th/U ratios mostly >0.1 (average 0.21). Fifteen analyses were conducted on 15 grains and yielded ages ranging from 112.0 to 123.0 Ma with mean $^{206}\text{Pb}/^{238}\text{U}$ ages of 116.0 ± 1.4 Ma (MSWD=2.4), which was interpreted as the crystallization age of the andesitic porphyrite.

The basalt sample Qg2 was sampled from 2 325 m deep of Well Qg2. Compared to the other 3 samples, zircon grains from sample Qg2 are much smaller (mostly $<100 \mu\text{m}$) and euhedral with a rhythmic oscillatory zoning structure (Fig. 5d). These grains have Th/U ratios ranging from 0.85 to 2.40 (average 1.78), a typical characteristic of magmatic zircon grains. Eleven analyses were conducted on 11 grains and produced ages ranging from 138.0 to 146.0 Ma with a mean $^{206}\text{Pb}/^{238}\text{U}$ age of 140.1 ± 1.4 Ma (MSWD=0.46) (Fig. 6d), which was interpreted as the crystallization age of the basalt.

4 DISCUSSION

The newly-obtained zircon U-Pb ages show that Jurassic magmatic rocks did not develop in the Huanghua depression, and the Cretaceous igneous rocks could be divided into two sets, namely, the Early Cretaceous and the Late Cretaceous (Table 1). Early Cretaceous igneous rocks are widely distributed in the north zone, with zircon U-Pb ages varying from 140 to about 112 Ma, lasted for about 30 Ma. The Late Cretaceous igneous rocks that was distributed in the south zone lasted from 75 to 70 Ma. In addition, Mesozoic granite only developed in the late stage and distributed sporadically in the Yanshan area to the east of the Wangquantun area. In summary, the early phase mainly developed intermediate-basic rocks, while the late phase developed intermediate-acid rocks.

4.1 Cretaceous Magmatic Activities of the Huanghua Depression

4.1.1 Early Cretaceous magmatic activities of the Huanghua depression

Based on zircon U-Pb data, lithology of the igneous rocks

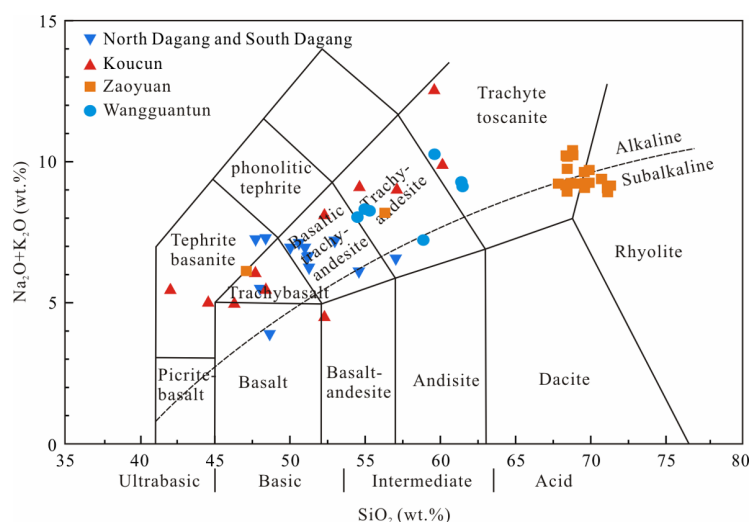


Figure 4. TAS diagram of the Cretaceous igneous rocks in Huanghua Depression. $\text{Na}_2\text{O}+\text{K}_2\text{O}$ versus SiO_2 after Le Bas et al. (1986), the dashed boundary between alkaline and subalkaline series after Irvine and Baragar (1971).

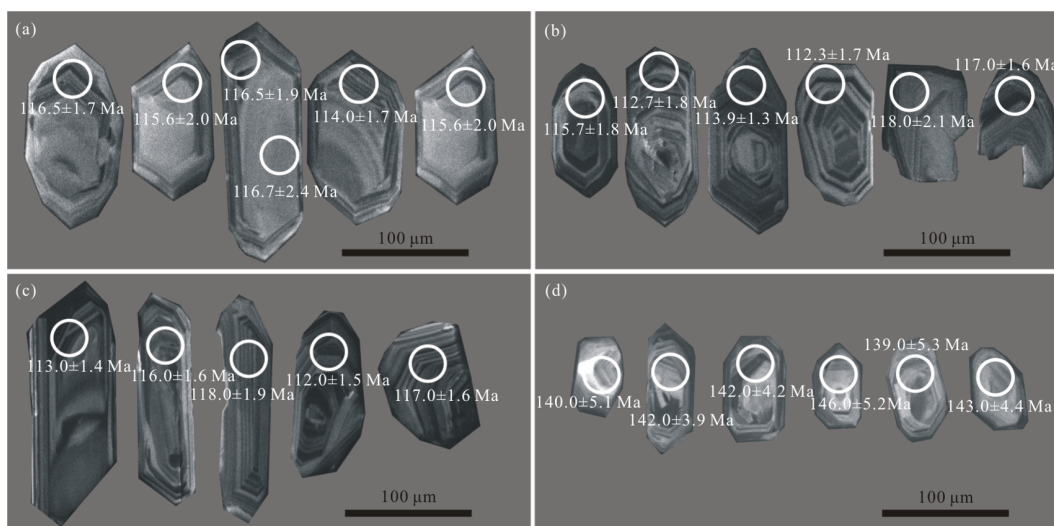


Figure 5. Cathodoluminescence (CL) images of typical zircons for the Cretaceous igneous rocks of the Huanghua depression. (a) Basalt of Well Qg101-1; (b) andesite of Well Qg101-2; (c) andesite porphyrite of Well Qg8; (d) basalt of Well Qg2. Circles and numbers denote analytical spots and correspondent ages, respectively.

and sedimentary layers, Zhu et al. (2019) subdivided the Early Cretaceous magmatism into two cycles. The early cycle formed between 125 and 120 Ma, while the late one lasted from 110 to 100 Ma. Moreover, an earlier cycle had been denuded before the 125–120 Ma cycle has been identified (Zhu et al., 2019). Combined with the newly-obtained data, we can divide the Early Cretaceous magmatism from the Huanghua depression into 3 cycles, in which cycle I happened in 140 Ma, cycle II between 125 and 119 Ma, and cycle III between 118 and 111 Ma (Fig. 7). The erosion of the Upper Cretaceous strata was recorded in all the wells, which is consistent with the previous conclusion that the Huanghua depression had experienced uplift and denudation in the Late Cretaceous (Wu et al., 2020).

Cycle I started at 140 Ma, with typical lithology of basalt that was only discovered in the North Dagang area. Guo et al. (2012) conducted zircon U-Pb dating on basalt sample from Well Qg2 and obtained the age of 133 ± 20 Ma. This age was calculated only based on four zircon grains and resulted in a large error of 20 Ma. Our newly-obtained zircon U-Pb age of

140.1 ± 1.4 Ma from basalt sample of 2 325 m depth is identical the age 139 Ma obtained from Gao and Zhang (1995) on basalt at the depth of 2 996 m. This implies that the two volcanic layers formed in a short period with about 700 m of sedimentary interval between them. Since there was no fault had been discovered in the thorough-Well Qg2 seismic section, we supposed the “basalt” sample tested by Gao and Zhang (1995) was either subvolcanic rock or hypabyssal intrusive rock such as basaltic porphyrite or diabase. Since the rock debris used in lithology naming were difficult to identify.

Cycle II was formed between 125 and 119 Ma and developed in the north zone, with dominant lithology of basalt, andesite, and volcanoclastic rocks. This cycle is mainly distributed in the Yangsanmu and Koucun areas. The typical wells X6 and K36 in Koucun represented the bottom-center and center-top parts of this cycle. The Well X6 developed andesite, basalt, and volcanoclastic rocks and tuff in the depths of 2 170–2 089, 2 039–2 016, and 1 796–1 778 m, respectively. The Well K36 developed interbedding of basalt and mudstone, volcanoclastic rocks and tuff,

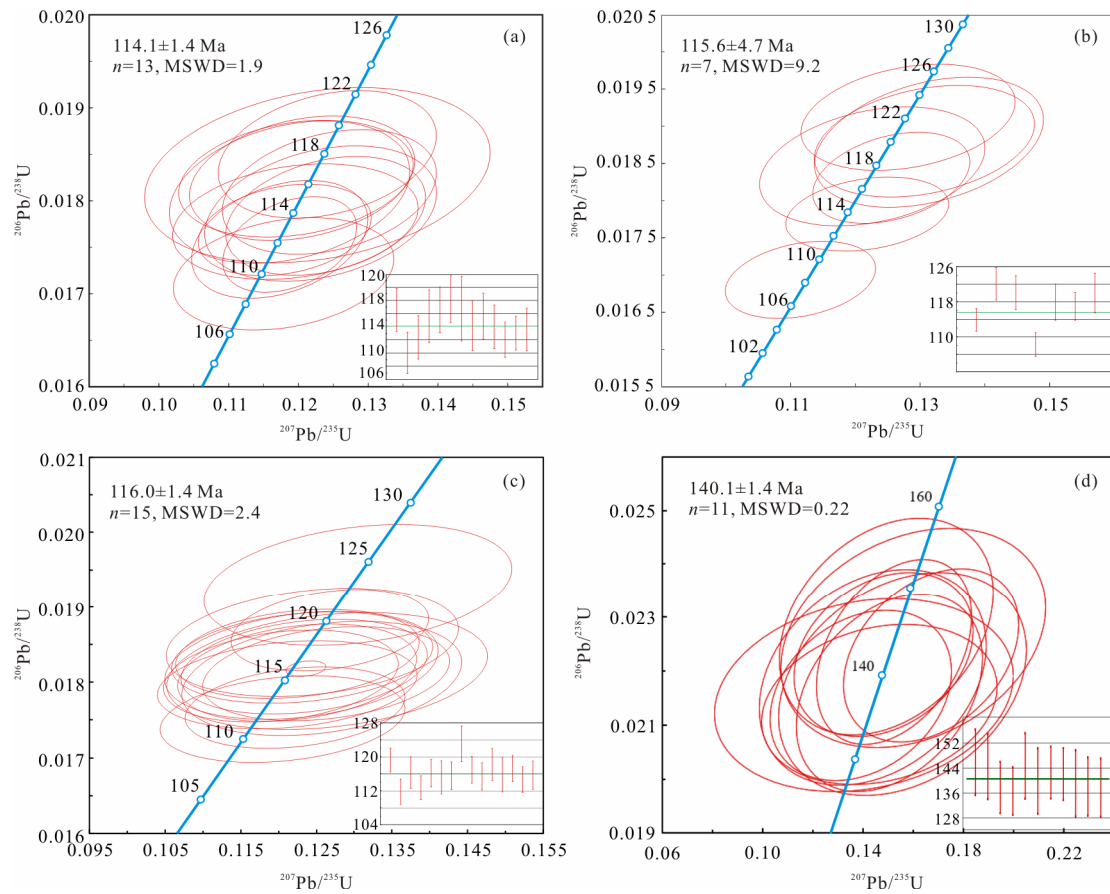


Figure 6. Zircon U-Pb concordia diagrams for the Cretaceous igneous rocks of the Huanghua depression. (a) Well Qg101-1, basalt; (b) Well Qg101-2, andesite; (c) Well Qg8, andesite porphyrite; (d) Well Qg2, basalt.

Table 1 Ages of Cretaceous igneous rocks in the Huanghua depression

Area	Well No.	Depth (m)	Lithology	Age (Ma)	Era	Data source
Yanshan	Y1	2 172	Granite	74.0±2.1	K ₂	*
Zaoyuan	Z1532	2 778	Andesite	72.0±1.9	K ₂	*
Zaoyuan	Z55	2 994	Andesite	75.77±2.02	K ₂	**
Zaoyuan	F22-15	2 950	Dacite-porphyrite	71.5±2.6	K ₂	Zhang et al. (2011)
Zaoyuan	F22-15	2 944	Dacite-porphyrite	69.95±0.78	K ₂	Zhu et al. (2019)
Zaoyuan	F22-15	2 956	Dacite-porphyrite	74.89±0.96	K ₂	Zhu et al. (2019)
Yanshanmu	Y23	1 525	Tuffite	111.46±0.76	K ₁	Zhu et al. (2019)
South Dagang	Qg101	3 198	Basalt	114.1±1.4	K ₁	This study
South Dagang	Qg101	3 150	Andesite	115.6±4.7	K ₁	This study
South Dagang	Qg8	3 373	Andesite	116.0±1.4	K ₁	This study
South Dagang	Qg1601	2 776	Tuffaceous sandstone	117.7±1.5	K ₁	Zhang F P et al. (2019)
Koucun	K23		Basalt	114.8±2.8	K ₁	Guo et al. (2012)
Koucun	K36	1 695	Andesite	118.8±1.0	K ₁	Zhang et al. (2011)
Koucun	K36	1 685	Andesite	123.4±2.2	K ₁	Zhang F P et al. (2019)
Xianzhuang	X6	1 776	Andesite	122.2±1.09	K ₁	Zhu et al. (2019)
Xianzhuang	X6	2 171	Volcanic breccia	123.1±1.09	K ₁	Zhu et al. (2019)
South Dagang	Qg2	2 325	Basalt	140.1±1.4	K ₁	This study
South Dagang	Qg2	2 996	Basalt	138.7±4.06	K ₁	Gao and Zhang (1995)
South Dagang	Qg2		Basalt	133±20	K ₁	Guo et al. (2012)

*. Unpublished data of Changqian Ma; **. unpublished data of Dagang Oilfield Company.

and andesite in the depths of 1 880–1 844, 1 784–1 826 and 1 666–1 760 m, respectively. The volcanoclastic breccia of Well X6 was dated at 122.2 ± 1.09 Ma by Zhu et al. (2019), and the andesite of Well K36 was dated at 123.4 ± 2.2 to 118.8 ± 1.0 Ma by Zhang F P et al. (2019) and Zhang et al. (2011). This indicates these rocks were formed in a very close time. The stratigraphic sequences of X6 and K36 show that medium-thick andesite and basalt layers are followed by thick layers of volcanoclastic rocks and tuff, and thick layers of andesite, it is indicated that the magma activity was a relatively quiet eruption and occasionally accompanied by an intensive explosive eruption.

Cycle III was formed between 118 and 111 Ma in the north zone too, mainly distributed in the South Dagang and North Dagang areas. Wells Qg8 and Qg101 are two new drillings and represent this cycle, which were drilled through the Mesozoic strata, unconformable contact with Permian due to the lack of the Jurassic and Triassic strata in the area. Basalt and andesite were recognized within the Cretaceous strata, whereas thick andesitic porphyrite were identified intruded into the Permian strata and dated at about 116 Ma. The igneous rocks developed near the unconformable contact interface of Cretaceous and Permian, which indicated the area may experience intensive denudation before cycle III.

Logging response is crucial for lithology identification and lithofacies classification of igneous rocks. The well and seismic data are important for fine stratigraphic division of volcanic reservoir (Chen et al., 2014). For instance, natural gamma ray (GR) and spontaneous potential (SP) curves change obviously at the lithologic boundaries of lava and sedimentary rocks, and the GR, SP and density curves are good indicators for stratigraphic correlation, lithology identification and facies classification of igneous rocks (Wang et al., 2015). Combined with the core samples and logging data, the characteristics of different cycles can be well constrained (Fig. 7).

In Well Qg2 of cycle I, the sedimentary rocks are brown siltstone and fuchsia siltstone interlayers in the bottom of the Cretaceous strata, with two thin beds of igneous rocks named basalt developed within brown siltstone layers. The GR curve shows obvious fluctuations where igneous rocks occurred. In the middle part, interbedding of thick brown siltstone, brown sandstone and fuchsia siltstone display smooth features of GR and SP curves. While near the top of Mesozoic strata, the GR curve displays regular and periodic changes caused by the multiple alternations of basalt and mudstone.

Wells X6 and K36 represent the lower and upper parts of cycle II, respectively. Gray andesite and basalt developed in the bottom of Well X6, and the relatively straight trend of GR and SP curves indicate the beginning of the cycle. Gray sandstone, siltstone and argillaceous sandstone show overall stable GR and SP trends in the middle part. The GR curve displays a rapid decreasing at the boundaries of the tuffs and sedimentary rocks, and the cycle rhythm occurred in the interior of andesite at the top of the cycle.

Cycle III also has distinct lithological association sequences and logging responses. Thick andesitic porphyrite intruded into the Permian strata with a stable trend of SP curve and periodic small amplitude changes of the GR curve. From the bottom up, the typical sequence is andesite with thin sedimentary rocks, then

follow by basalt and andesite layers, and thin tuff at last. The GR curve displays a trend from increasing to decreasing, and changing to increase at last, and the SP curve shows a periodic fluctuation at the andesite layers on the near top.

4.1.2 Late Cretaceous magmatic activities of the Huanghua depression

In contrast to the Early Cretaceous, the Late Cretaceous mainly developed intermediate and acid igneous rocks. The principal lithologies include andesite, dacite porphyrite and granite. The andesite and dacite porphyrite were concentrated in the Zaoyuan and Wangguantun areas, and granite was developed in the Yanshan area, with typical wells of Z1532, F22-15, G177, and Y1 (Fig. 8) from the south of the study area.

Both andesite from Well Z1532 and dacite porphyrite from Well F22-15 formed at about 72 Ma. The Wangguantun area is located to the southeast of the Zaoyuan area and separated by the Kongxi fault, where the typical Well G177 developed thick layers of andesite. Since only one set of andesite has been identified in the south zone, we proposed that the andesite of Well G177 belongs to the Late Cretaceous. The Well Y1 within the Yanshan area was drilled into about 900 m thick granite from depth 1 300 to 2 200 m but did not drill through Mesozoic strata after the well completion, the U-Pb dating of granite is 74.0 ± 2.1 Ma. Granite is rarely developed in Late Cretaceous granite in the study area and even in the North China Craton, so it could be an important indicator for our understanding of the magmatic activity.

The current available data show that the wells in the Zaoyuan area share many similarities with those in the Wangguantun area. For instance, they all are lack of the top of Cretaceous strata, and none drillings have drilled into the Early Cretaceous igneous rocks, and also, drilled through the Mesozoic strata. The presence of the Late Cretaceous volcanic rocks indicates that the south zone had suffered less erosion than the north zone, which caused the Early Cretaceous igneous rocks buried even deeper than the current drilling depth in the south zone.

The lithological association sequences and logging responses are simple in the Late Cretaceous magmatism. The GR curves are stable for granite within Well Y1 and andesite within Well Z1532, while the decrease at the top of dacite porphyrite within Well F22-15 may indicate the effect of the lithology boundary with sedimentary rock on it. The GR and SP curves in Well G177 have periodic changes, which are mainly caused by the small differences of magma composition of eruption rhythms.

4.2 Cretaceous Magmatism and Igneous Reservoirs of Huanghua Depression and Contrast with Adjacent Areas

In the following, Early Cretaceous magmatism and reservoirs developed in Bohai Sea area, Liaoning Province and Huanghua depression are discussed. Late Cretaceous magmatism and reservoirs developed in the Jiaolai Basin, Liaohe depression and Huanghua depression are discussed (Fig. 9).

4.2.1 Early Cretaceous magmatism and igneous reservoirs of Huanghua depression and contrast with adjacent areas

Previous studies suggested that the subsidence-uplift during Mesozoic were related to the subduction and rollback of

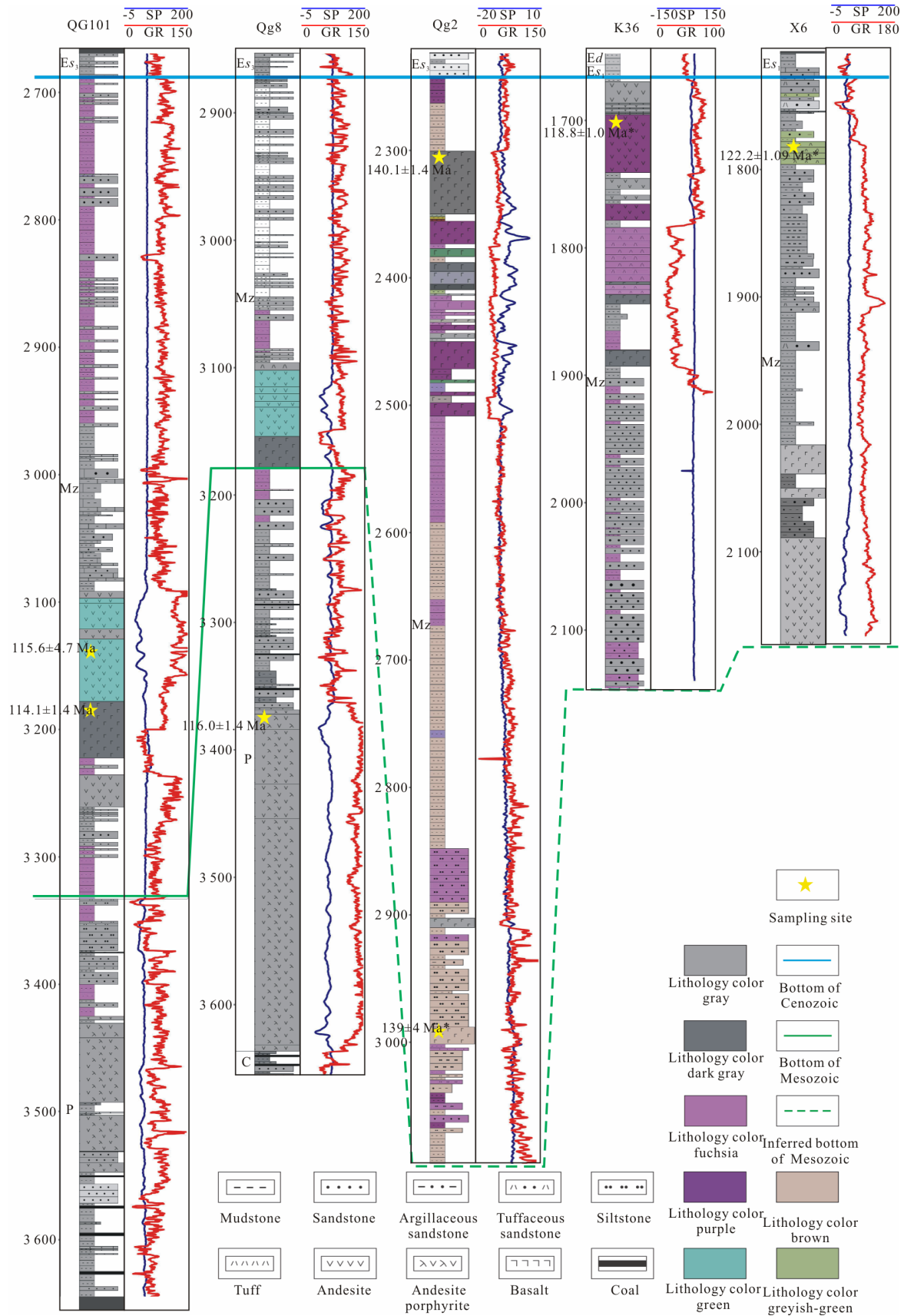


Figure 7. Lateral comparison chart of the Early Cretaceous igneous rocks in the Huanghua depression. The chart agrees with line 1 in Fig. 1, data sources correspond to Table 1. Well Qg2 represents the characteristics of cycle I, wells K36 and X6 represent the characteristics of cycle II, wells Qg101 and Qg8 represent the characteristics of cycle III, respectively. SP. Spontaneous potential logging; GR. natural gamma ray logging; Mz. Mesozoic; P. Permian; C. Carboniferous; Es₁, Es₃. the first and the third members of Eocene Shahejie Formation; Ed. the Eocene Dongying Formation.

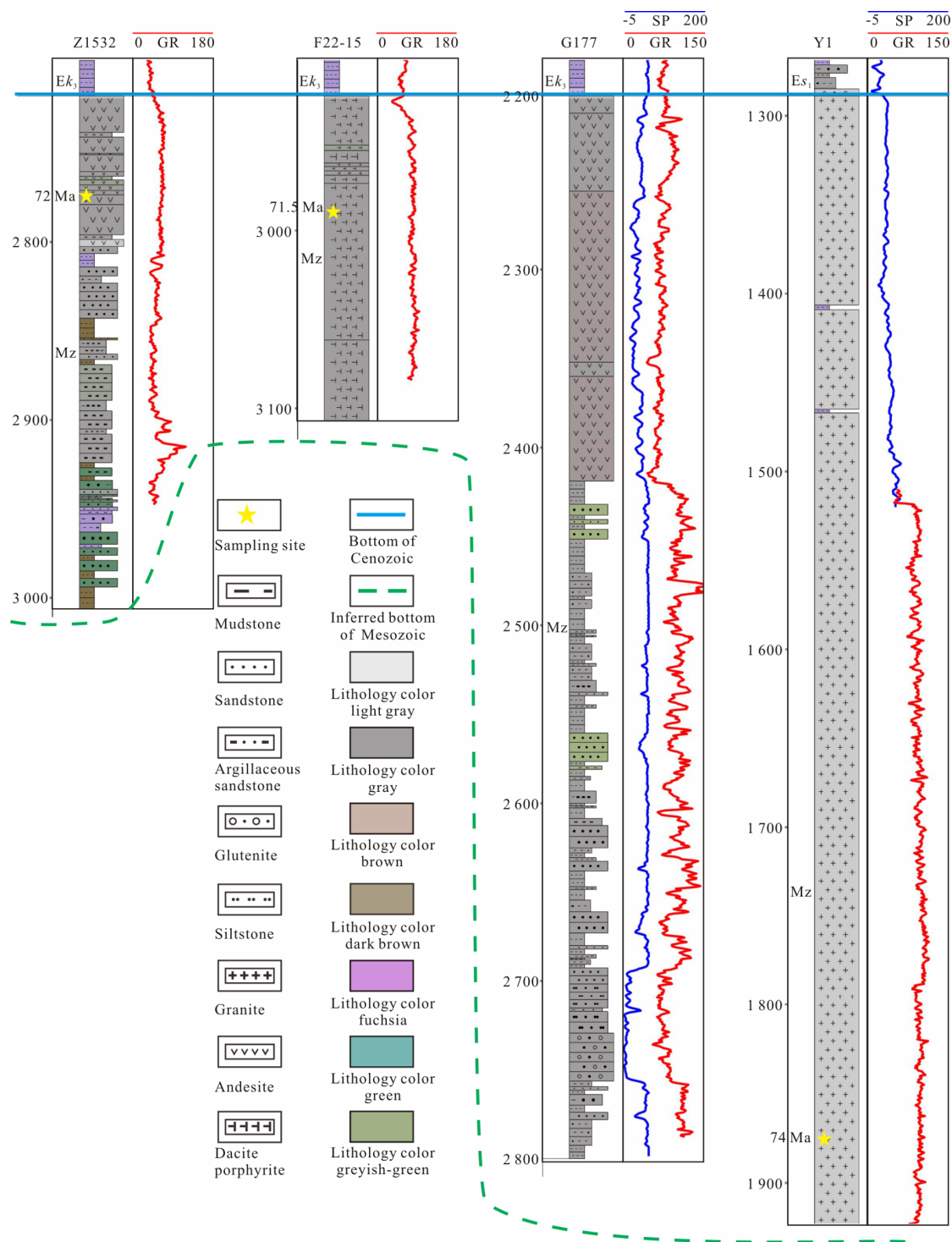


Figure 8. Lateral comparison chart of the Late Cretaceous igneous rocks in Huanghua depression. The chart agrees with line 2 in Fig. 1, data sources correspond to Table 1. SP. Spontaneous potential; GR. natural gamma ray. *Ek₃*. the third member of Eocene Kongdian Formation; Mz. Mesozoic.

the paleo-Pacific Plate (Zhang et al., 2011; Li et al., 2010). Although with a similar tectonic setting, igneous rocks in the Bohai Bay Basin are significantly different from West Liaoning Province. One of the important distinctions is the lack of the Tuchengzi Formation and Zhangjiakou Formation commonly developed in West Liaoning Province, which could be attributed to the uplift of Bohai Bay Basin in the Late Jurassic (Zhu et al., 2019).

The comparison study of the Mesozoic magmatism in

Huanghua depression, Bohai Sea with those from West Liaoning Province shows that the Early Cretaceous magmatism of Huanghua depression may correlate with the Yixian Formation of the other two areas. The lateral comparison chart (Fig. 9) shows that there are three or four cycles of magmatism developed in different areas, which can be subdivided by igneous rock assemblages and sedimentary layers.

The typical geological section of Yixian Formation in West Liaoning Province has been divided into 4 cycles. The

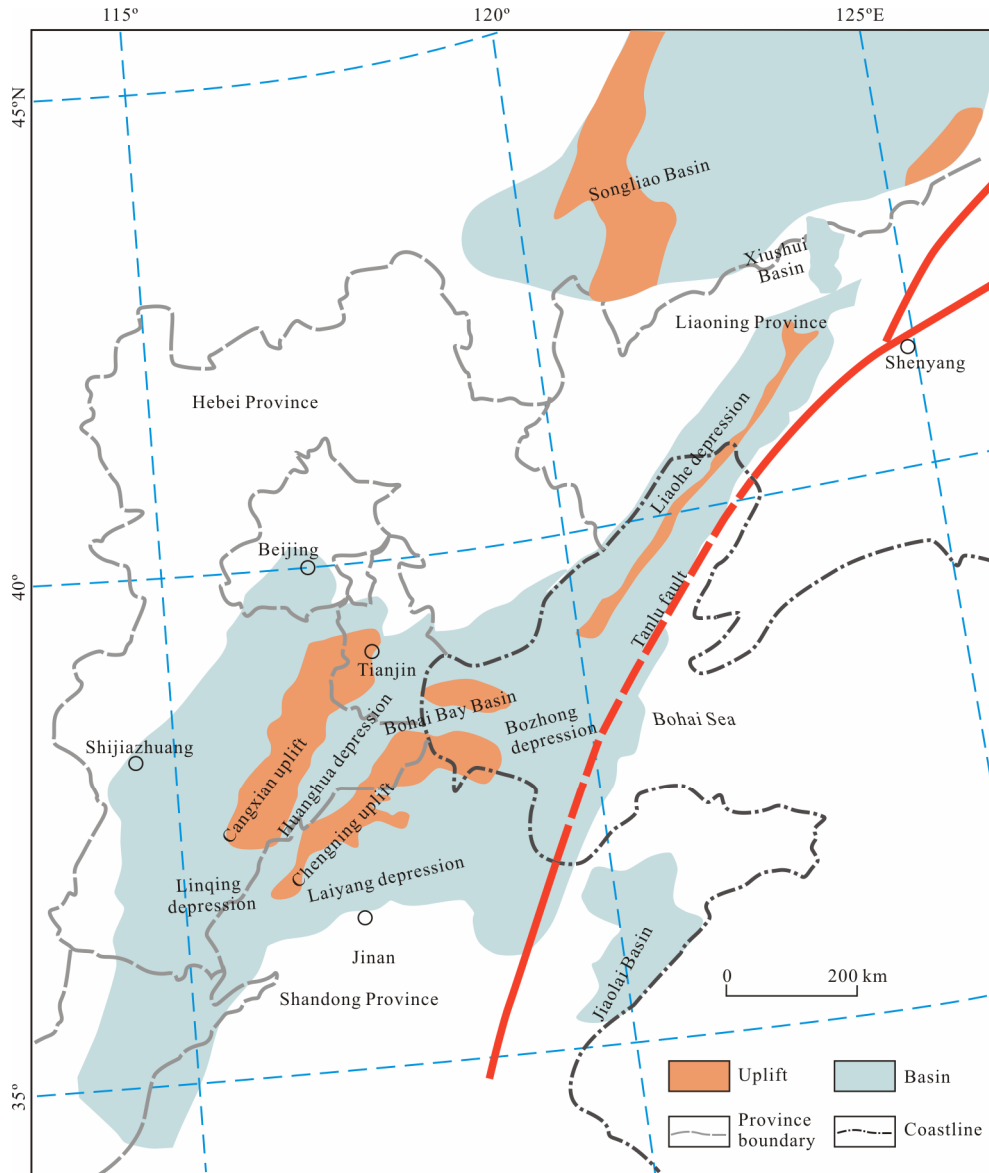


Figure 9. Sketch map of Huanghua depression and adjacent areas showing the basin with Cretaceous igneous reservoirs in North China.

stratification boundaries including Zhuanchengzi bed, Dakangbao bed and Jingangshan bed, basic and intermediate rocks were developed in cycle I and cycle II, whereas intermediate and acid rocks were developed in cycle III and cycle IV, respectively (Ding et al., 2019; Zhang H et al., 2008).

The nature and formation of the Yixian Formation in the Bohai Sea is poor constrained because it lies on the seafloor. The evidence from the drillings (Cai et al., 2018; Wu et al., 2017; Ye et al., 2017) resulted in a stratigraphic column of the Early Cretaceous igneous rocks in the Bohai Sea area (Fig. 10). Wu et al. (2017) suggested that there were 3 cycles of magmatism developed in the Early Cretaceous, which started from 128 Ma. However, the basalt below the earliest rocks they studied has not been dated yet. According to the regional data, lithologic composition, and deposition sequence, we proposed that there are 4 cycles of magmatism developed in the Bohai Sea area, which is contrasted with that in Liaoning Province. We hold the point that the 3 cycles of magmatism proposed by Wu et al. (2017) identified are the later 3 cycles in the Early

Cretaceous, while the basalt below the 128 Ma basalt layer is the first cycle magmatic activity in the area. From cycle I to cycle IV, the lithological sequence in the Bohai Sea display a similar trend as observed in West Liaoning Province, but the volcanoclastic rocks have not been identified in cycle I and the magmatism lasted longer in cycle IV in the Bohai Sea area.

In the Huanghua depression, the general characteristics of lithologic variation trend in the Early Cretaceous are similar to that of the Yixian Formation in the other two areas, but the magmatic sequence is different at some extent. The magmatism in the Huanghua depression could be subdivided into 3 cycles discussed before, therein with similarities between the first two cycles to those from the other two areas, but the main differences are the presence of basalt and the absence of acid rocks in cycle III.

The following discussion of magmatism and igneous reservoirs are based on the magmatic sequences of Huanghua depression, wherein the cycles III and IV of Liaoning Province and Bohai Sea areas are seen as a whole to compare with cycle III of

Huanghua depression.

The cycle I developed in the Lower Cretaceous and is mainly composed of basalt and andesite. Although the ages of basalts of the cycle I in the Bohai Sea area is unavailable, the geological evidence shows that the basalts were formed earlier than 128 Ma. The ages of basalt and andesite are dated to be 136 and 132.3–131.5 Ma in West Liaoning, respectively (Zhang et al., 2016; Cai et al., 2010; Chen and Chen, 1997). Combined with the newly obtained zircon U-Pb age of 140.1 Ma on basalt from Well Qg2 in this study, we proposed that the cycle I magmatism activities in these areas share with very similar ages regardless their slightly different lithologies. Basalt is the most widespread lithology of this cycle in the three locations we compared, and volcanoclastic rocks and andesite only developed in Liaoning Province. According to the current exploration, no hydrocarbon accumulation has been recognized related to all the igneous rocks in this cycle.

Cycle II is the main stage of magmatism in Yixian Formation and well-studied. The U-Pb ages of Yixian Formation in West Liaoning Province, Bohai Sea area and in Huanghua depression range from 129.7–122 (Cai et al., 2010; Zhang H et al., 2008, 2005; Wu et al., 2017) to 123.4–118.8 Ma (Zhu et al., 2019; Zhang et al., 2011). The lithological association reflects the alternativity of magmatic eruption, effusion, and sedimentation in this cycle. The magmatism in the Huanghua depression occurred later than the West Liaoning and Bohai Sea areas, and a larger scale of explosive facies rocks developed in the Bohai Sea area and Huanghua depression. The intensive volcanic activities in this cycle resulted to thick layers of vesicular basalt and andesite and formed reservoir space for oil and gas.

Cycle III is the last stage of Early Cretaceous magmatism in the North China Craton, with ages varying from 123–111 (Zhu et al., 2019; Guo et al., 2012; Xiao et al., 2008; Zhang H et al., 2008, 2005) to 118–108 Ma (Wu et al., 2017) in Liaoning Province, Bohai Sea and Huanghua depression. The intermediate and acid rocks are the principal igneous rocks developed in this cycle, with similar lithologies in different areas. The except is the lack of acid rocks in the Huanghua depression. It should be pointed out that the thick andesitic porphyrite developed in the South Dagang of Huanghua depression, which is an important sign for cycle III in the depression.

Based on three drillings of Early Cretaceous in the Xiushui Basin located in Liaoning Province, Ding et al. (2019) suggested that the volcanic rocks in cycle II and sedimentary rocks in cycle III were the major reservoirs, the mudstone in cycle III has good hydrocarbon bearing conditions. The igneous reservoirs are mainly andesite and volcanoclastic rocks in cycle II. This is similar to Liaoning Province. Wu et al. (2017) found that the intermediate-acid rocks developed at the top of cycle III have better oil-gas show than the other sub cycles. They proposed that the lithology is the main factor for different oil-gas bearing grades in different cycles and the porosities of intermediate-acid rocks were better than basic rocks, which may have been caused by the dissolution of anhydrites. In Huanghua depression, we found that the igneous reservoirs are principally intermediate rocks with a few tuffs and volcanic sedimentary rocks in cycle II and basic-intermediate rocks in cycle III, while no oil-gas show within the basalt beds in cycle I and cycle II. Moreover, the an-

desite reservoirs of the Well Qg8 is a typical rich reservoir type in North Dagang area.

To summarize, intensive magmatism has a closer relationship to the reservoirs, since the cycle II and cycle III are the good reservoirs in the Early Cretaceous in the basins of North China Craton. Considering their spatial and temporal distribution, the intermediate-acid rocks in cycle II and the basic rocks in cycle III are the main reservoirs in the north zone of the Huanghua depression, and the cycle III is worthy of further study for future exploration.

4.2.2 Late Cretaceous magmatism and igneous reservoirs of Huanghua depression and contrast with adjacent areas

The Late Cretaceous magma activity in the North China Craton was weak and poorly-constrained, with the ages mainly concentrated in 86 and 70 Ma. The zircon U-Pb ages of Jiaolai Basin in Shandong Province, the Liaohe depression in Liaoning Province, and the Huanghua depression are 86–72 (Zhang J et al., 2008; Meng et al., 2006; Yan et al., 2005), 82–70 (Kuang et al., 2012; Wang et al., 2006; Bing et al., 2003) and 75.7–71.5 Ma (Zhu et al., 2019; Zhang et al., 2011), respectively (Fig. 11). The lithologies of these areas are different from each other. The Jiaolai Basin is mainly composed of basalt and diabase and the Liaohe depression principally developed basalt, dacite, with a small amount of volcanoclastic rocks, while the Huanghua depression developed intermediate-acid rocks and lithology including granite, andesite, volcanoclastic rocks, dacite porphyry, with a small amount of basalt. The igneous rocks in Huanghua depression have more complex lithologies and concentrated zircon U-Pb ages relatively to the other two areas.

According to the early studies and our new data, the reservoirs are mainly related to the intermediate-acid rocks in this stage. There are no oil or gas reservoirs related to the Late Cretaceous basalt in the Jiaolai Basin. Meng et al. (2006) found that the thickness of Late Cretaceous basalt was only about 10 m, and the upper and lower layers were thick sandstone beds. Liu and Wu (2007) suggested that the Cretaceous igneous rocks in the Jiaolai Basin could provide heat source and promote the hydrocarbon generation for the underlying Laiyang Formation and acted as caprocks for the reservoirs. The thick igneous rocks and sandstones stopped the upward migration of oil and gas stored in Laiyang Formation, and the thick overlying layers of sandstone made the Late Cretaceous igneous rocks to be non-reservoir beds.

In Liaohe depression, the dominant igneous hydrocarbon reservoirs were located in the Xinglongtai area and is dominated by andesite and dacite. It has been proposed that the lithology is one of the main controlling factors for reservoirs (Li et al., 2012; Mu et al., 2005). The case studies on the Mesozoic igneous reservoirs in Dawa area in the southeast of Liaohe depression (Li et al., 2020) showed that the effusive basalt have bad storage physical properties. By contrast, basaltic breccia rocks were excellent reservoirs because of their mass of interbreccia pores and vesicles. In Huanghua depression, several case studies on the igneous rocks of the Zaoyuan and Wangquantun areas (Gao et al., 2015) suggested that the principal reservoirs were the vesicular andesite layers that commonly developed at the top or bottom of the volcanic apparatus

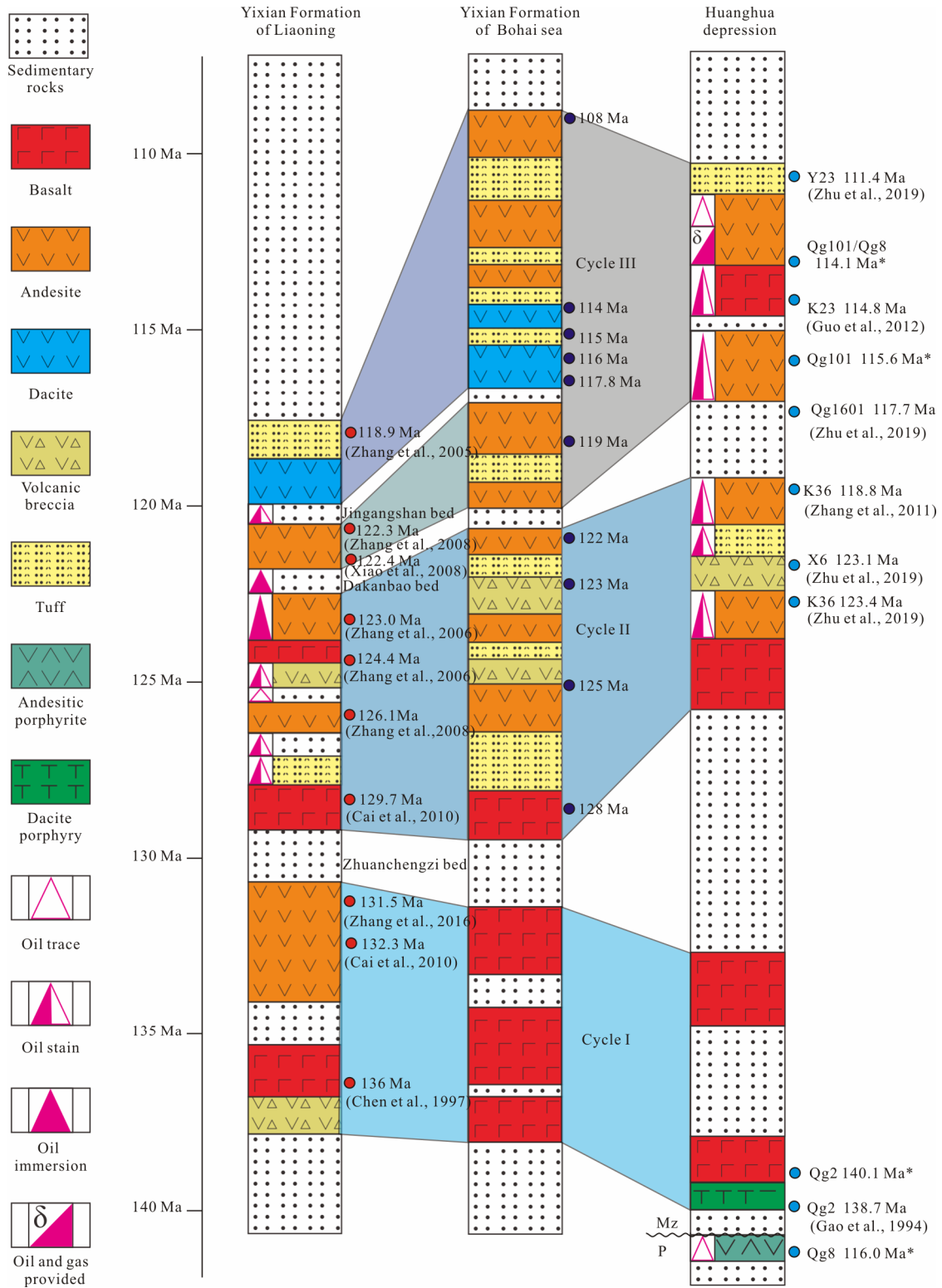


Figure 10. Lateral comparison chart of the typical Early Cretaceous igneous rocks of Huanghua depression and its surrounding areas (145–108 Ma). Intermediate-acid rocks and volcanic sedimentary rocks were the main reservoirs in cycle II and cycle III. Data of the Bohai Sea from Wu et al. (2017), data with * from this study. P. Permian; Mz. Mesozoic.

(Wang et al., 2004). This study shows that the dacite porphyry and a few volcanic sedimentary rocks are also important reservoirs in the Late Cretaceous, in which the tectonic fractures act as migration pathways and also storage spaces for oil and gas.

4.3 Hydrocarbon Enrichment Characteristics of the Cretaceous Igneous Rocks in Huanghua Depression

Many researchers investigated the main controlling factors of igneous reservoirs, such as the relationship between igneous rocks and source rocks, the influence among tectonic fault zones,

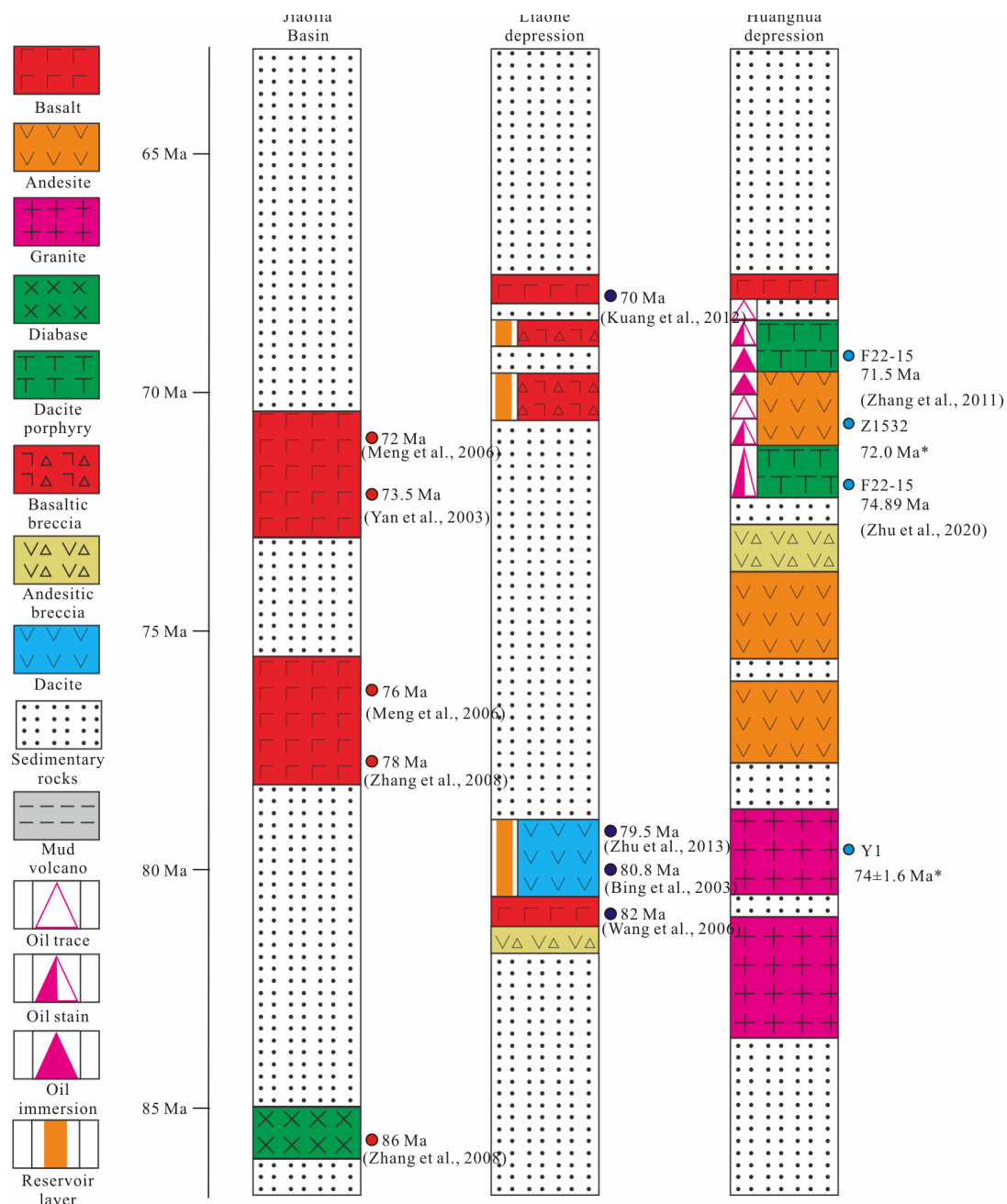


Figure 11. Lateral comparison chart of the typical Late Cretaceous igneous rocks of Huanghua depression and its surrounding areas (86–65 Ma). Intermediate and acid rocks were the principal hydrocarbon accumulation reservoirs in Late Cretaceous. *. Unpublished data of Changqian Ma.

lithologies and lithofacies and their reservoir space, the weathering and leaching effects to reservoir spaces (Zheng et al., 2018; Ye et al., 2017). Previous studies on the Bohai Bay Basin and Huanghua depression proposed that the oil and gas were mainly formed in Cenozoic, and the Mesozoic igneous reservoirs have typical characteristics of “young source in the old reservoir” (Zheng and You, 2019; Jin et al., 2012). Jin et al. (2012) summarized three typical hydrocarbon reservoir types to explain how Cenozoic oil and gas charge into Mesozoic igneous rocks in the Bohai Bay Basin, including buried hill type, fault-block type and stratigraphic-lithologic type, in which the first two types are closely related to the faults formed by tectonic activities. In addition, the deep fractures provided channels for the migration of light oil and gas and the small cracks caused by local tectonic

movements can also connect the original isolated primary pores and further increased the permeability of rocks (Siler et al., 2018). In short, tectonic activities and faults have been confirmed to have an important influence on hydrocarbon enrichment in “young source in the old reservoir” type reservoirs, which may apply equally to the igneous reservoirs in the Huanghua depression. Hence, we are not going to discuss the significance of fault in isolation in this study, but pay more attention to the relationships of the reservoirs with lithology and reservoir spaces.

4.3.1 Oil-gas bearing grades of different lithologies in the Huanghua depression

Fourteen Early Cretaceous wells and 20 Late Cretaceous wells with oil-gas shows associated with igneous rocks were

summarized, and the relationships of reservoir thickness with lithology and oil-bearing grades are shown in Fig. 12.

In the Early Cretaceous, basalt and andesite dominate the reservoirs. Basalt reservoirs, with a total thickness of >230 m, occupy the largest proportion of igneous reservoirs, in which >50% show fluorescence, >30% show oil trace and <10% show oil stain. Andesite layers occupy a thickness of about 50 m and mainly show fluorescence. The share of volcanic sedimentary and tuff are significantly lower than basalt and andesite, though most of the tuff show higher oil-gas bearing grade (Figs. 12a and 12b). The basalt and andesite reservoirs were developed in both cycle II and cycle III (Fig. 10), which were the periods of maximum magmatic activities in the Early Cretaceous. Thus, we proposed that the intensive magmatism more conducive to the formation of reservoirs. Besides, the basalt developed in cycle I and cycle II have no oil-gas show in Huanghua depression (Fig. 10). Therefore, we suggested the basalt in cycle III has large exploration potential in the Early Cretaceous in the Huanghua depression.

In the Late Cretaceous, dacite porphyrite layers are the most developed igneous rock with oil-gas shows, the total thickness is >700 m with >70% of them characterized by oil-bearing grades higher than fluorescence. Andesite has a total thickness of >200 m with most of them show fluorescence. The thickness of volcanoclastic rocks and volcanic sedimentary are <100 m (Figs. 12c and 12d). Obviously, dacite-porphyrinite could be considered as the key exploration objects in the Late Cretaceous due to its thickness and higher grades of oil-gas bearing grades than andesite, and volcanic sedimentary layers are worthy of attention because more than 90% of them show higher grade.

In summary, the intensive Early Cretaceous magmatism

may have played a key role in formation of these reservoirs, and basalt in cycle III could be the best exploration target, dacite-porphyrinite could be considered as the key exploration object.

4.3.2 Characteristics and controlling factors of oil and gas reservoir spaces in Huanghua depression

Because the oil-gas reservoir spaces directly affect the quality of the petroleum reservoirs of igneous rocks, many researchers have discussed the influence factors to the reservoirs, such as lithologies, lithofacies, tectonic and diagenetic effects and the development of the weathering crust (Wang Y et al., 2018; Zheng et al., 2018). Lithological and lithofacies differences result in different types and intensities of pores. The primary vesicles and fractures laid the foundation for the development and transformation of effective reservoirs. The secondary processes of epidiagenesis are also the key factors, such as weathering and leaching. The formation fluid dissolution can significantly modify the petrophysical characteristics of the reservoir rocks. Meanwhile, tectonism is necessary for the formation of reservoir spaces and the migration, permeation, and accumulation of oil and gas (Zheng et al., 2018; Mao et al., 2015).

For equivalent eruption conditions, the silicic samples show higher tortuosities and produce smaller vesicle sizes and lower permeabilities than mafic samples (Heather et al., 2009). For instance, basalt usually developed larger vesicles than andesites in the core samples in Huanghua depression (Figs. 13a–13c, 13g–13i). If they have similar contact relations with source rocks, primary vesicles, and fractures of basalt could have higher permeabilities and provide better reservoir spaces than andesite, which can explain the basalt has better oil-gas bearing grades than the andesite in the Early Cretaceous.

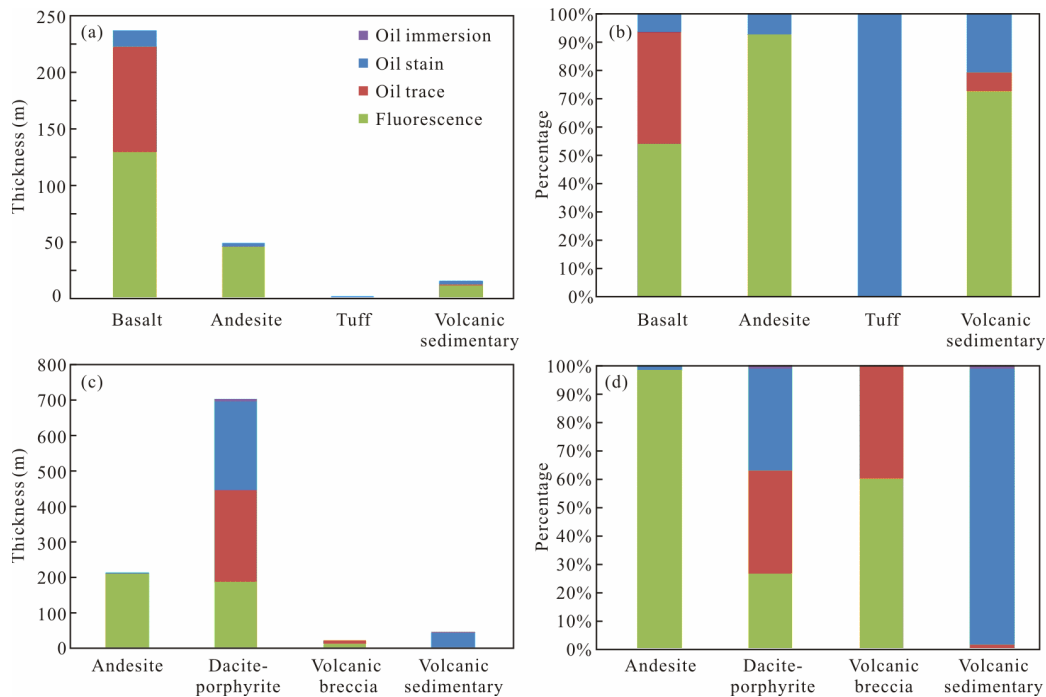


Figure 12. Oil-bearing grades of Cretaceous igneous rocks of Huanghua depression. (a) Total thickness for Early Cretaceous igneous rocks with oil-gas shows; (b) percentage of oil-gas bearings grades for different lithologies of Early Cretaceous; (c) total thickness for Late Cretaceous igneous rocks with oil-gas shows; (d) percentage of oil-gas bearing grades for different lithologies of Late Cretaceous.

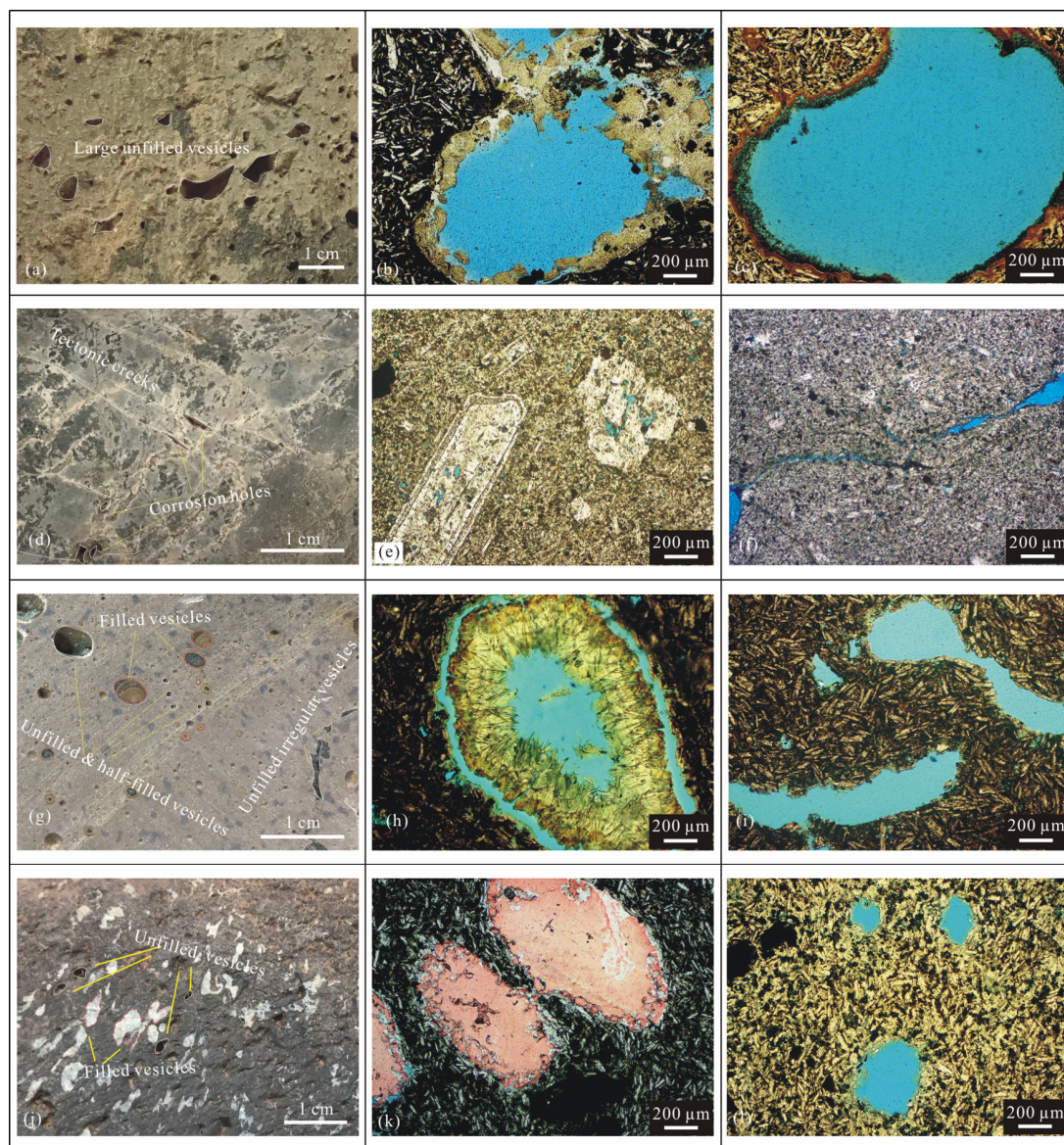


Figure 13. Different reservoir spaces of igneous rocks. (a), (d), (g), (j) Core images, others are casting thin sections. (a) Well J21-23, 1 589.76 m, large vesicles of basalt; (b) Well J21-23, 1 582.64 m, small amount filled vesicles of basalt; (c) Well J21-23, 1 590.22 m, unfilled vesicles of basalt; (d) Well F22-15, 2 965.26 m, tectonic fractures and corrosion holes of dacite porphyry; (e) Well F22-15, 2 941.37 m, intercrystalline pores of K-feldspar phenocrysts of dacite porphyry; (f) Well F22-15, 2 982.79 m, tectonic cracks of dacite porphyry; (g) Well G177, 2 309.35 m, different types of unconnected vesicles of andesite; (h) Well G177, 2 309.18 m, half-filled vesicle of andesite; (i) Well G177, 2 309.18 m, irregular vesicles of andesite; (j) Well W6, 2 573.25 m, two types of unconnected vesicles of andesite; (k) Well W6, 2 568.73 m, amygdaloidal andesite; (l) Well W6, 2 578.05 m, small vesicles of andesite.

As mentioned above, the basalt reservoirs were concentrated in cycle III, then why the basalts in cycle I and cycle II were a failure of accumulation? As shown in Figs. 7 and 10, thick sedimentary rocks are laid above the cycle I basalt, so if there were no large faults to connect the basalt with Cenozoic source rocks, it's hard for oil and gas to charge into the basalt. As a matter of fact, there was no contact relationship between the cycle I igneous rocks and hydrocarbon source rocks have been discovered yet. For cycle II, andesite and tuff developed certain reservoirs, similar to cycle I, no basalt reservoir was discovered as well. Since only a few core samples have been obtained, we suggest two possible reasons. One possible explanation is that the basalt of this cycle lacks good storage spaces; while the other is the andesite above the basalt has

vesicles and dense zones. As a result, the oil and gas would trap in the vesicle zone and formed a reservoir, but the dense zone cut off the migration channel to the basalt. To clarify that, more work related to the 3D seismic interpretation and logging data analysis should be done in the future.

In the Late Cretaceous, the main lithologies of reservoir rocks are dacite porphyry and andesite, and dacite porphyry show better oil-gas bearing characteristics than andesite in the study area (Fig. 12). Casting thin sections show the andesite created different types of primary vesicles, but because few tectonic fractures were developed, most of the vesicles were unconnected. Meanwhile, many vesicles were fully filled with hydrothermal minerals by a secondary process (Figs. 13g–13l), which led to the failure of migration and accumulation of oil

and gas. On the contrary, dacite porphyry hardly created vesicles but developed a lot of tectonic fractures, hydrothermal fluid can be transferred through the fractures and dissolved the feldspars, and at last formed inter-crystalline pores and corrosion holes (Figs. 13d–13f). Finally, oil and gas were charged into the secondary pores through the tectonic fractures and formed reservoirs.

5 CONCLUSIONS

(1) The Huanghua depression developed two sets of Cretaceous igneous rocks and the Early Cretaceous magmatism mainly developed in the north zone with basic and intermediate rocks, while the late one developed in the south with acid and intermediate rocks.

(2) The Early Cretaceous magmatism in the Huanghua depression occurred in 140–112 Ma and could be subdivided into 3 cycles, with the ages of 140, 125–119, and 118–111 Ma, respectively. GR and SP curves are clearly distinguishable in lithology identification and lithofacies division. They have obvious fluctuations at the interfaces of igneous and sedimentary rocks and could be seen as evidence of cycles division. Compared with magmatism of Yixian Formation in Liaoning Province and the Bohai Sea area, the cycle I magmatism was small scale, whereas cycle II and cycle III magmatism activity were much stronger with repeated effusive and explosive phases.

(3) The late set magmatism of the Huanghua depression was short-lived with the age of 75–70 Ma. Compared with the igneous rocks of the similar period in the Jiaolai Basin and Liaohe depression, the Huanghua depression developed more complex lithology and formed in a shorter time. Intermediate and acid rocks were the main reservoirs in the Late Cretaceous in the Huanghua depression and the Liaohe depression.

(4) Intensive magmatism in the Early Cretaceous is crucial to the formation of reservoirs, as evidenced by the fact that the basalt in cycle III has good reservoir spaces and large exploration potential. In the Late Cretaceous, hydrothermal fluid migrated through the tectonic fractures, dissolved the feldspars and formed abundance of secondary pores, making the dacite porphyrite to be key exploration objects in this period.

ACKNOWLEDGMENTS

This study was jointly supported by the PetroChina Dagang Oilfield Company (No. DGTU-2018-JS-408), the National Petroleum Corporation Major Science and Technology Program of China (No. 2018E-11). The authors sincerely appreciate Prof. Xuan-Ce Wang for his English polishing, and the reviewers and the editors for their suggestions. The final publication is available at Springer via <https://doi.org/10.1007/s12583-020-1308-8>.

REFERENCES CITED

- Bing, Z. B., Liu, W. H., Huang, Z., et al., 2003. Stratigraphy Sequence and Age of the Upper Cretaceous Daxingzhuang Formation in West Liaoning Province. *Geological Bulletin of China*, 22(5): 351–355 (in Chinese with English Abstract)
- Cai, D. M., Ye, T., Lu, F. T., et al., 2018. Lithofacies Characteristics and Identification Methods of Mesozoic Volcanic Rocks in Bohai Sea. *Lithological Reservoirs*, 30(1): 112–120 (in Chinese with English Abstract)
- Cai, H. A., Xu, D. B., Li, B. F., et al., 2010. A Study on Early Cretaceous Volcanic Effusion Periods and Isotope Chronology in Western Liaoning. *Coal Geology of China*, 22(12): 1–6 (in Chinese with English Abstract)
- Chen, H. Q., Hu, Y. L., Jin, J. Q., et al., 2014. Fine Stratigraphic Division of Volcanic Reservoir by Uniting of Well Data and Seismic Data. *Journal of Earth Science*, 16(2): 337–347. <https://doi.org/10.1007/s12583-014-0424-8>
- Chen, Y. X., Chen, W. J., 1997. Volcanic Rocks in Western Liaoning and Its Adjacent Areas. Seismological Press, Beijing (in Chinese)
- Ding, Q. H., Chen, S. W., Li, X. H., 2019. Geological Characteristics and Oil-Bearing Prospect of Lower Cretaceous in Xiushui Basin of Northern Liaoning Province. *Geological Survey of China*, 6(3): 14–21 (in Chinese with English Abstract)
- Dong, S. W., Zhang, Y. Q., Li, H. L., et al., 2018. The Yanshan Orogeny and Late Mesozoic Multi-Plate Convergence in East Asia—Commemorating 90th Years of the “Yanshan Orogeny”. *Science China Earth Sciences*, 61: 1888–1909. <https://doi.org/10.1007/s11430-017-9297-y>
- Feng, Z. H., Yin, C. H., Liu, J. J., et al., 2014. Formation Mechanism of *in-situ* Volcanic Reservoirs in Eastern China: A Case Study from Xushen Gasfield in Songliao Basin. *Science China: Earth Sciences*, 44: 2221–2237 (in Chinese)
- Fu, L. X., Lou, D., Li, H. J., et al., 2016. Control Effect of Indosinian Yanshan Movement on the Formation of Buried Hill in Dagang Exploration Area. *Acta Petrolei Sinica*, 37(S2): 19–30 (in Chinese with English Abstract)
- Gao, Y., Su, L. P., Wang, L., et al., 2015. Identification of Volcanic Rocks and Reservoir Beds by Well Logging in Southern Oilfields of Dagang Prospect. *Special Oil and Gas Reservoirs*, 22(4): 66–70 (in Chinese with English Abstract)
- Gao, Z. Y., Zhang, L. C., 1995. Volcanic Rocks and Oil and Gas Reservoir. Northwest University, Xi'an
- Gong, Z. S., Cai, D. S., Zhang, G. C., 2007. Dominating Action of Tanlu Fault on Hydrocarbon Accumulation in Eastern Bohai Sea Area. *Acta Petrolei Sinica*, 28(4): 1–10 (in Chinese with English Abstract)
- Gu, L. X., Ren, Z. W., Wu, C. Z., et al., 2002. Hydrocarbon Reservoirs in a Trachyte Porphyry Intrusion in the Eastern Depression of the Liaohe Basin, Northeast China. *AAPG Bulletin*, 86(10): 1821–1832
- Guo, Y. F., 2012. Petrology and Geochemistry of Mesozoic-Cenozoic Igneous Rocks in Huanghua Depression and the Formation Mechanism: [Dissertation]. Northwest University, Xi'an (in Chinese with English Abstract)
- He, D. F., Ma, Y. S., Liu, B., et al., 2019. Main Advances and Key Issues for Deep-Seated Exploration in Petroliferous Basin in China. *Earth Science Frontiers*, 26(1): 1–12 (in Chinese with English Abstract)
- Heather, M. W., Katharine, V. C., Emily, H. G., et al., 2009. Pore Structure of Volcanic Clasts: Measurements of Permeability and Electrical Conductivity. *Earth and Planetary Science Letters*, 280(1–4): 93–104. <https://doi.org/10.1016/j.epsl.2009.01.023>
- Hu, Z. C., Zhang, W., Liu, Y. S., et al., 2015. “Wave” Signal Smoothing and Mercury Removing Device for Laser Ablation Quadrupole and Multiple Collector ICP-MS Analysis: Application to Lead Isotope Analysis. *Analytical Chemistry*, 87(2): 1152–1157. <https://doi.org/10.1021/ac503749k>
- Irvine, T. N., Baragar, W. R. A., 1971. A Guide to the Chemical Classification to the Common Volcanic Rocks. *Canadian Journal of Earth Sciences*, 8(5): 523–548. <https://doi.org/10.1139/e71-055>
- Jin, C. S., Pan, W. L., Qiao, D. W., et al., 2013. Volcanic Facies and Their Reservoirs Characteristics in Eastern China Basins. *Journal of Earth Science*, 24(6): 935–946. <https://doi.org/10.1007/s12583-013-0380-8>
- Jin, C. S., Qiao, D. W., Dan, W. N., 2012. Meso-Cenozoic Volcanic Rock Distribution and Reservoir Characteristics in the Bohai Bay Basin. *Oil and Gas Geology*, 33(1): 19–36 (in Chinese with English Abstract)
- Kuang, Y. S., Wei, X., Hong, L. B., et al., 2012. Petrogenetic Evaluation of the

- Laohutai Basalts from North China Craton: Melting of a Two-Component Source during Lithospheric Thinning in the Late Cretaceous–Early Cenozoic. *Lithos*, 54: 68–82. <https://doi.org/10.1016/j.lithos.2012.06.027>
- Le Bas, N. J., Le Maitre, R. W., Streckeisen, A., et al., 1986. A Chemical Classification of Volcanic Rocks Based on the Total Alkali-Silica Diagram. *Journal of Petrology*, 27(3): 745–750. <https://doi.org/10.1093/ptrology/27.3.745>
- Li, H. N., Gao, R. J., Zhang, H. D., 2020. Characteristics and Hydrocarbon Accumulation Models of Mesozoic Volcanic Reservoirs in Dawa Area in the Liaohe Depression. *Geology in China*. <http://kns.cnki.net/kcms/detail/11.1167.P.20200116.1505.006.html>
- Li, J., Yang, G. D., Fang, B. Z., et al., 2012. Research Status of Igneous-Rock Reservoir Exploration in Liaohe Oilfield. *Journal of Oil and Gas Technology*, 34(7): 45–53 (in Chinese with English Abstract)
- Li, S. W., Wu, Y. P., Liu, H. Q., et al., 2014. Characteristics and Distribution of Oil Reservoirs Related to Cenozoic Igneous Rocks in Qikou Depresson. *Journal of Jilin University: Earth Science Edition*, 44(4): 1071–1084 (in Chinese with English Abstract)
- Li, S. Z., Suo, Y. H., Dai, L. M., et al., 2010. Development of the Bohai Bay Basin and Destruction of the North China Craton. *Earth Science Frontiers*, 17(4): 64–89 (in Chinese with English Abstract)
- Liu, J., Wu, C. L., 2007. Characteristics and Geologic Meaning of the Magmatic Activities in Jiaolai Basin. *Petroleum Geology and Oilfield Development in Daqing*, 26(5): 36–40 (in Chinese with English Abstract)
- Liu, Y. S., Gao, S., Hu, Z. C., et al., 2010. Continental and Oceanic Crust Recycling-Induced Melt-Peridotite Interactions in the Trans-North China Orogen: U-Pb Dating, Hf Isotopes and Trace Elements in Zircons of Mantle Xenoliths. *Journal of Petrology*, 51(1/2): 537–571. <https://doi.org/10.1093/ptrology/egp082>
- Luo, J. L., Qu, Z. H., Sun, W., et al., 1996. The Relations between Lithofacies Reservoir Lithology and Oil and Gas of Volcanic Rocks in Fenghuadian Area. *Acta Petrolei Sinica*, 17(1): 32–39 (in Chinese with English Abstract)
- Luo, X., Gong, S., Sun, F. J., et al., 2017. Effect of Volcanic Activity on Hydrocarbon Generation: Examples in Songliao, Qinshui, and Bohai Bay Basins in China. *Journal of Natural Gas Science and Engineering*, 38: 218–234. <https://doi.org/10.1016/j.jngse.2016.12.022>
- Ma, X. H., Yang, Y., Zhang, J., et al., 2019. A Major Discovery in Permian Volcanic Rock Gas Reservoir Exploration in the Sichuan Basin and Its Implications. *Natural Gas Industry B*, 6(4): 419–425. <https://doi.org/10.1016/j.ngib.2019.02.001>
- Mao, Z. G., Zhu, R. K., Luo, J. L., et al., 2015. Reservoir Characteristics, Formation Mechanisms and Petroleum Exploration Potential of Volcanic Rocks in China. *Petroleum Science*, 12 (1): 54–66. <https://doi.org/10.1007/s12182-014-0013-6>
- Meng, F. C., Li, T. F., Xue, H. M., et al., 2006. Two Stories of Basic Magmas from Different Mantle Sources of Late Cretaceous in East Shandong Province, China: A comparative Study on Basalts from Zhucheng and Jiaozhou. *Acta Petrological Sinica*, 22(6): 1644–2656 (in Chinese with English Abstract)
- Mu, D. L., Li, C., Liu, J. Y., 2005. Mesozoic Igneous Reservoir Forecast and Exploration Achievements in Niuxintuo Area, Liaohe Depressio. *Petroleum Exploration and Development*, 32(3): 67–69 (in Chinese with English Abstract)
- Mu, D., 2015. Methods Research on Lithology Identification for Intermediate/Basaltic Rocks in Liaohe Basin: [Dissertation]. Jilin University, Changchun (in Chinese with English Abstract)
- Schutter, S. R., 2003. Occurrences of Hydrocarbons in and around Igneous Rocks. *Geological Society, London, Special Publications*, 214(1): 35–68. <https://doi.org/10.1144/gsl.sp.2003.214.01.03>
- Siler, D. L., Hinz, H. N., Faults, E. J., 2018. Stress Concentration at Structural Discontinuities in Active Fault Zones in the Western United States: Implications for Permeability and Fluid Flow in Geothermal Fields. *Geological Society of America Bulletin*, 130(7/8): 1273–1288. <https://doi.org/10.1130/b31729.1>
- Wang, G., Qing, Y., Shen, J., et al., 2018. Dynamic-Change Laws of the Porosity and Permeability of Low- to Medium-Rank Coals under Heating and Pressurization Treatments in the Eastern Junggar Basin, China. *Journal of Earth Science*, 29(3): 607–615. <https://doi.org/10.1007/s12583-017-0908-4>
- Wang, H. C., Ran, Q. Q., Hu, Y. L., 2004. Igneous Lithofacies in Zao 35 Block, Dagang Oilfield. *Petroleum Exploration and Development*, 31(5): 22–24 (in Chinese with English Abstract)
- Wang, P. J., Chen, S. M., 2015. Cretaceous Volcanic Reservoirs and Their Exploration in the Songliao Basin, Northeast China. *AAPG Bulletin*, 99(3): 499–523. <https://doi.org/10.1306/09041413095>
- Wang, W., Xu, W. L., Ji, W. Q., et al., 2006. Late Mesozoic and Paleogene Basalts and Deep-Derived Xenocrysts in Eastern Liaoning Province, China: Constraints on Nature of Lithospheric Mantle. *Geological Journal of China Universities*, 12(1): 30–40 (in Chinese with English Abstract)
- Wang, Y., Yang, R. C., Song, M. S., et al., 2018. Characteristics, Controls and Geological Models of Hydrocarbon Accumulation in the Carboniferous Volcanic Reservoirs of the Chunfeng Oilfield, Junggar Basin, Northwestern China. *Marine and Petroleum Geology*, 94: 65–79. <https://doi.org/10.1016/j.marpetgeo.2018.04.001>
- Wang, Z. H., Zhu, X. M., Sun, Z. C., et al., 2015. Igneous Lithology Identification and Lithofacies Classification in the Basin Using Logging Data: Taking Junggar Basin as an Example. *Earth Science Frontiers*, 22(3): 254–268 (in Chinese with English Abstract)
- Wen, L., Li, Y., Yi, H. Y., et al., 2019. Lithofacies and Reservoir Characteristics of Permian Volcanic Rocks in the Sichuan Basin. *Natural Gas Industry B*, 6(5): 452–462. <https://doi.org/10.1016/j.ngib.2019.02.003>
- Wong, W. H., 1929. The Mesozoic Orogenic Movement in Eastern China since Mesozoic Time. *Bulletin of the Geological Society of China*, 8(1): 33–44. <https://doi.org/10.1111/j.1755-6724.1929.mp8001004.x>
- Wu, Q. X., Wang, Y. C., Wei, A. J., et al., 2017. Division of the Mesozoic Volcanic Rock Eruption Cycle and Its Relationship with Oil and Gas in the Bohai Sea. *China Offshore Oil and Gas*, 29(2): 18–26 (in Chinese with English Abstract)
- Wu, Z. P., Zhang, F. P., Li, W., et al., 2020. Apatite Fission Track Evidence of Mesozoic Tectonic Evolution in the Huanghua Depression. *Journal of China University of Mining and Technology*, 49(1): 131–144 (in Chinese with English Abstract)
- Xiao, G. Q., Gao, S., Huang, H., et al., 2008. Zircon U-Pb Geochronology and Geochemistry of Mesozoic Volcanic Rocks from Dasijiazhi Area at Zhangwu, West Liaoning Province. *Earth Science*, 33(2): 151–164 (in Chinese with English Abstract)
- Xie, Y. H., Luo, X. P., Wang, D. Y., et al., 2019. Hydrocarbon Accumulation of Composite-Buried Hill Reservoirs in the Western Subsag of Bozhong Sag, Bohai Bay Basin. *Natural Gas Industry B*, 6(6): 546–555. <https://doi.org/10.1016/j.ngib.2019.05.002>
- Yan, J., Chen, J. F., Xie, Z., et al., 2005. Studies on Petrology and Geochemistry of the Late Cretaceous Basalts and Mantle-Derived Xenoliths from Eastern Shandong. *Acta Petrologica Sinica*, 21(1): 99–112 (in Chinese with English Abstract)
- Yang, C., Hou, L., Yang, F., et al., 2017. Controlling Factors of Volcanic Hydrocarbon Reservoirs in Bohai Bay Basin, China. *Journal of Natural Gas Science*, 2(4): 219–228. <https://doi.org/10.1016/j.jnggs.2017.10.001>
- Ye, T., Wei, A. J., Zhu, C. R., et al., 2017. Characteristics of the Basement

- Reformed Volcanic Edifice in Bohai Sea and Its Implication for Hydrocarbon Enrichment. *Petroleum Research*, 2(4): 336–346. <https://doi.org/10.1016/j.ptlrs.2017.10.001>
- Zhang, C., Ma, C. Q., Liao, Q. A., et al., 2009. Geochemistry of Late Mesozoic–Cenozoic Volcanic Rocks in the Huanghua Depression, Bohai Bay: Petrogenesis and Implications for Tectonic Transition. *Acta Petrologica Sinica*, 25(5): 1159–1177 (in Chinese with English Abstract)
- Zhang, C., Ma, C. Q., Liao, Q. A., et al., 2011. Implications of Subduction and Subduction Zone Migration of the Paleo-Pacific Plate beneath Eastern North China, Based on Distribution, Geochronology, and Geochemistry of Late Mesozoic Volcanic Rocks. *International Journal of Earth Sciences*, 100(7): 1665–1684. <https://doi.org/10.1007/s00531-010-0582-6>
- Zhang, F. P., Wu, Z. P., Li, W., et al., 2019. Structural Characteristics and Its Tectonic Evolution of Huanghua Depression during the Indosinian–Yanshanian. *Journal of China University of Mining and Technology*, 48(4): 842–857 (in Chinese with English Abstract)
- Zhang, H., Guo, W. M., Liu, X. M., et al., 2008. Constraints on the Late Mesozoic Regional Angular Unconformity in West Liaoning–North Hebei by LA-ICP-MS Dating. *Progress in Natural Science*, 18(11): 1395–1402. <https://doi.org/10.1016/j.pnsc.2008.05.013>
- Zhang, H., Liu, X. M., Chen, W., et al., 2005. The Age of the Top of the Yixian Formation in the Beipiao–Yixian Area, Western Liaoning, and Its Importance. *Geology in China*, 34(4): 596–603 (in Chinese with English Abstract)
- Zhang, H., Liu, X. M., Yuan, H. L., et al., 2006. U–Pb Isotopic Age of the Lower Yixian Formation in Lingyuan of Western Liaoning and Its Significance. *Geological Review*, 52(1): 63–71 (in Chinese with English Abstract)
- Zhang, J. L., He, S., Wang, Y. Q., et al., 2019. Main Mechanism for Generating Overpressure in the Paleogene Source Rock Series of the Chezheng Depression, Bohai Bay Basin, China. *Journal of Earth Science*, 30(4): 775–787. <https://doi.org/10.1007/s12583-017-0959-6>
- Zhang, J. N., Fu, L. X., Zhou, J. S., et al., 2019. Macroscopic Distribution Characteristics and Evolution Process of Buried Hill in the Huanghua Depression, Bohai Bay Basin. *Acta Geologica Sinica*, 93(3): 585–596 (in Chinese with English Abstract)
- Zhang, J., Zhang, H. F., Ying, J. F., et al., 2008. Contribution of Subducted Pacific Slab to Late Cretaceous Mafic Magmatism in Qingdao Region, China: A Petrological Record. *Island Arc*, 17(2): 231–241. <https://doi.org/10.1111/j.1440-1738.2008.00612.x>
- Zhang, Q., Zhang, M. S., Li, X. B., et al., 2016. Stratigraphic Sequences and Zircon U–Pb Dating of Yixian Formation in Caozhuang Area of Xingcheng, Western Liaoning. *Global Geology*, 35(1): 51–65 (in Chinese with English Abstract)
- Zhang, Z. K., Ling, M. X., Lin, W., et al., 2020. “Yanshanian Movement” Induced by the Westward Subduction of the Paleoe-Pacific Plate. *Solid Earth Sciences*, 5(2): 103–114. <https://doi.org/10.1016/j.sesci.2020.04.002>
- Zhao, Y., Xu, G., Zhang, S. H., et al., 2004. Yanshanian Movement and Conversion of Tectonic Regimes in East Asia. *Earth Science Frontiers*, 11(3): 319–328 (in Chinese with English Abstract)
- Zheng, H., Sun, X. M., Zhu, D. F., et al., 2018. Characteristics and Factors Controlling Reservoir Space in the Cretaceous Volcanic Rocks of the Hailar Basin, NE China. *Marine and Petroleum Geology*, 91: 749–763. <https://doi.org/10.1016/j.marpetgeo.2018.01.038>
- Zheng, Q. H., You, J. Y., 2019. Hydrocarbon Accumulation Characteristics of Cretaceous Volcanic Rocks in Wangguantun Tectonic Zone, Huanghua Depression. *Lithologic Reservoirs*, 31(5): 44–51 (in Chinese with English Abstract)
- Zhou, L. H., Fu, L. X., Lou, D., et al., 2012. Structural Anatomy and Dynamics of Evolution of the Qikou Sag, Bohai Bay Basin: Implications for the Destruction of North China Craton. *Journal of Asian Earth Sciences*, 47: 94–106. <https://doi.org/10.1016/j.jseae.2011.06.004>
- Zhou, L. H., Qin, M. T., Xiao, D. Q., et al., 2020. Multiscale Properties of 2D Reservoir Micropore Heterogeneity Based on Digital Casting Thin Sections Images. *Natural Resources Research*. <https://doi.org/10.1007/s11053-020-09747-8>
- Zhu, G., Wang, D. X., Liu, G. S., et al., 2004. Evolution of the Tanlu Fault Zone and Its Responses to Plate Movement in West Pacific Basin. *Chinese Journal of Geology*, 39(1): 36–49 (in Chinese with English Abstract)
- Zhu, J. C., Feng, Y. L., Meng, Q. R., et al., 2019. Late Mesozoic Tectonostratigraphic Division and Correlation of Bohai Bay Basin: Implications for the Yanshanian Orogeny. *Science China Earth Sciences*, 62(11): 1783–1804. <https://doi.org/10.1007/s11430-018-9382-7>
- Zong, K. Q., Klemd, R., Yuan, Y., et al., 2017. The Assembly of Rodinia: The Correlation of Early Neoproterozoic (ca. 900 Ma) High-Grade Metamorphism and Continental arc Formation in the Southern Beishan Orogen, Southern Central Asian Orogenic Belt (CAOB). *Precambrian Research*, 290: 32–48. <https://doi.org/10.1016/j.precamres.2016.12.010>
- Zou, C. N., Zhang, G. Y., Zhu, R. K., et al., 2013. Exploration History and Features of Volcanic Reservoirs. In: Zou, C. N., ed., *Volcanic Reservoirs in Petroleum Exploration*. Elsevier Science, Burlington. 1–10.
- Zuo, Y. H., Qiu, N. S., Li, J. W., et al., 2015. Meso-Cenozoic Tectono-Thermal Evolution History in Bohai Bay Basin, North China. *Journal of Earth Science*, 26(3): 352–360. <https://doi.org/10.1007/s12583-014-0500-0>